UNIVERSIDADE DO ALGARVE

DEPARTAMENTO DE CIÊNCIAS BIOMÉDICAS E MEDICINA

CELLULAR BEHAVIOUR OF NEURONAL AND GLIA CELLS IN ELECTRONIC DEVICES

ANA LUÍSA GARCIAS MESTRE

Dissertação de Mestrado em Ciências Biomédicas

Trabalho efetuado sob a orientação de:

Orientador: Prof. Doutor Henrique Leonel Gomes

Coorientadora: Prof. Doutora Inês Araújo

2015

UNIVERSIDADE DO ALGARVE
DEPARTAMENTO DE CIÊNCIAS BIOMÉDICAS E MEDICINA

CELLULAR BEHAVIOUR OF NEURONAL AND GLIA CELLS IN ELECTRONIC DEVICES

ANA LUÍSA GARCIAS MESTRE

Dissertação de Mestrado em Ciências Biomédicas

Trabalho efetuado sob a orientação de:

Orientador: Prof. Doutor Henrique Leonel Gomes
Coorientadora: Prof. Doutora Inês Araújo

2015

Declaração de autoria de trabalho

Declaro ser o autor deste trabalho, que é original e inédito. Autores e trabalhos consultados estão devidamente citados no texto e constam da listagem de referências incluída.

_____

(Ana Luísa Garcias Mestre)

Copyright © Ana Mestre, 2015

"A Universidade do Algarve tem o direito, perpétuo e sem limites geográficos, de arquivar e publicitar este trabalho através de exemplares impressos reproduzidos em papel ou de forma digital, ou por qualquer outro meio conhecido ou que venha a ser inventado, de o divulgar através de repositórios científicos e de admitir a sua cópia e distribuição com objetivos educacionais ou de investigação, não comerciais, desde que seja dado crédito ao autor e editor".

Agradecimentos

A Universidade do Algarve tornou-se uma segunda casa por mim, como tal, o meu primeiro agradecimento vai exatamente para este grande centro de partilha de conhecimento que me acompanha há cerca de 8 anos.

A concretização deste trabalho não teria sido possível sem ajuda crucial de um conjunto de pessoas cuja colaboração e apoio foi essencial para a realização deste trabalho final. Por ter estado inserida em dois laboratórios distintos, tenho que agradecer a todos os meus colegas do laboratório de Biologia Molecular da Universidade do Algarve, em especial à Natércia que me acompanhou desde a minha chegada até à data e claro, à Professora Leonor Cancela que me acompanhou também desde o inicio da minha carreira, me proporcionou estar onde estou hoje, assim como por sempre se mostrar disponível para me ajudar e tentando ao máximo que abrisse os meus horizontes.

Queria agradecer aos meus colegas do laboratório de Engenharia Electrónica com quem trabalho diariamente, que se tornaram de certa forma família. Pedro, Joana (Té), Sanaz, Vitaly, Cardoso, Fábinho, Lino e Valdemira não só por toda a ajuda que me deram, mas também pela boa companhia e pelo precioso ambiente que todos juntos conseguimos criar dia após dia.

Não posso deixar de agradecer especialmente ao Pedro, que sem ele esta interface entre a electrónica e a biologia não teria acontecido, ou pelo menos, não desta forma tão benéfica. Quero-lhe agradecer também pela disponibilidade e amizade. Foi muito bom poder contar sempre com ele em qualquer circunstância.

Queria deixar um agradecimento especial também à minha querida amiga e colega Joana Canudo (Té) por tudo. Fez parte da minha vida tanto académica como pessoal e cuja força, empenho e ajuda foi essencial também para a realização deste trabalho.

A todos meus amigos que sem eles também não poderia ser possível terminar este trabalho cujo espaço se torna bastante reduzido para enumerar cada um deles, tendo a certeza que sabem quem são, o meu muitíssimo obrigada por terem feito comigo esta jornada que agora se aproxima do final, sem vocês não teria conseguido.

Aos meus irmãos, Miguel e João, que sem dúvida são grandes responsáveis pela pessoa que me tornei hoje. A amizade e amor incondicional que partilhamos tiveram um papel indispensável para que conseguisse chegar até aqui.

Ao Ricardo que me acompanhou nesta fase tão crucial, stressante e importante da minha vida, por acreditar e me dar força, por me receber sempre com um sorriso rasgado na cara mesmo quando eu sabia que era apenas para me ver sorrir. Por me ter feito sorrir todos estes intensos e prolongados meses o meu muito obrigada.

À minha mãe, sem dúvida! Muito obrigada, muito obrigada as vezes que forem necessárias. A pessoa que me ensinou a ser quem eu sou hoje, cujas palavras de encorajamento foram fundamentais, não esquecendo abraços intensos e fortes foram tão

importantes para que chegasse a esta fase com força e garra de continuar. Quem me ensinou mesmo quando nada parece correr bem o amor incondicional supera tudo.

Ao meu pai por estar presente nos momentos importantes da minha vida, pelos ensinamentos, pela generosidade, assim como pelo enorme apoio. Por acreditar que consigo e pelo exemplo de sempre nos deu.

À Professora Inês Araújo por todo o apoio, sabedoria, pela oportunidade, críticas fundamentais, disponibilidade e calma manifestada para me orientar neste percurso tão importante.

Por fim, gostaria de agradecer ao Professor Henrique, não só pela ajuda crucial, como também a amizade que fez questão de partilhar e, não só ao longo deste ano lectivo que passou, pelo qual eu estava destinada a realizar esta dissertação, mas principalmente pelos últimos 3 anos onde se mostrou sempre muito acessível, preocupado e determinado a me ensinar a crescer como pessoa e como profissional. Por todas as portas que me ajudou a abrir e por me ensinar a "abrir a mente" para novos horizontes. Por me mostrar novos caminhos e ensinar-me que desistir não faz parte do vocabulário. Fez-me aprender a lidar com o verdadeiro significado de "stress" e saber que se nos esforçarmos no final vai tudo correr bem. Entre discussões também houve muitas gargalhadas que valeram a pena cada segundo porque acaba por nos conseguir ensinar sempre algo. Por fim, não posso deixar de lhe agradecer por me ter mostrado o verdadeiro significado da palavra líder e de tentar exprimir o orgulho que possuo por os nossos caminhos se terem cruzado.

Gostaria também de agradecer a todo o apoio financeiro de "European Community Seventh Framework Programme" (FP7/2007-2013) através do projeto iONE-FP7 grant agreement n° 280772 e da Fundação para a Ciência e Tecnologia (FCT), através do projeto "Intelligent Cell Surfaces (ICS)", refº EuroBioSAS/0001/2010.

Resumo

O objetivo desta tese foi estudar o comportamento celular em células neurais em dispositivos electrónicos criando uma ponte entre a electrónica e a biologia. Para este trabalho, células neurais (Neuro-2a) e células da glia (C6) foram cultivadas numa diversidade de componentes electrónicos. Um grande número de dispositivos protótipos foram fabricados e optimizados para interagir com diferentes tipos de células. O tempo de vida, a sensibilidade do componente e o desempenho global foram também avaliados. Foram utilizadas técnicas elétricas de forma a monitorizar as células *in vitro*, como medições da impedância eléctrica de forma a adquirir informação acerca da adesão celular e viabilidade.

As experiências realizadas forneceram conhecimentos fundamentais: como medir sinais celulares eléctricos utilizado bioelectrónica e também como desenvolver novos transdutores com aplicação nas ciências vivas. Também surgiram aplicações interessantes aplicadas ao mesmo ramo, como é o caso de criar uma plataforma de rastreio de drogas.

Por fim, foi também possível observar sinais quase periódicos que nós supomos tratarem-se de ondas de cálcio intracelulares. Com esta tese, foi possível optimizar materiais e dispositivos para fabricar dispositivos electrónicos capazes de adquirir biosinais extracelulares muito fracos.

Este trabalho está integrado no Projecto Europeu iONE-FP7[1] cujo objetivo é criar um componente para reparar lesões na medula espinhal.

O componente dá-se pelo nome de "Active Multifunctional Implantable Device" - AMID. O AMID é fabricado numa estrutura biocompatível e biodegradável. O objetivo do grupo de investigação da Universidade do Algarve é desenvolver e optimizar componentes individuais antes de serem incorporados no AMID.

Lesão na medula espinhal é uma doença neurodegenerativa que afecta aproximadamente 4 milhões de pessoas em todo o mundo. Esta doença é caracterizada pela desconexão dos axónios, perda de neurónios e de células da glia e desmielinização associada a um processo degenerativo de inflamação secundária relacionado com extensão variável da área lesionada e, como tal, encontra-se relacionada também com diferentes défices funcionais.

[1] http://ione-fp7.eu/consortium/

Palavras-chave: Componente electrónico Implantável, Cultura de células, Células C6, Células Neuro-2a, Impedância, Plataforma de drogas, Ondas de Cálcio.

Abstract

The aim of this thesis was to study the cellular behaviour of neural cells in electronic devices by creating a bridge between electronics and biology. With this purpose in mind, neuronal cells (Neuro-2a) and glioma C6 cells were cultured in a diversity of electronic devices. A large number of prototypes devices were fabricated and optimized to interact with different types of cells. The lifetime, the sensitivity of the device, and the overall performance were assessed. Electrical techniques were used to monitor cells *in vitro*, such as impedance measurements of weak signal to acquire information about cell adhesion and viability.

The experiments performed were fundamental to understand how to measure cellular electrical signals using bioelectronics and how to develop new transducers with applications in life sciences. Interesting side-ways applications have emerged, for instance, for drug screening platforms.

Finally, it was also possible to observe "quasi-periodic" signals that we advance to be intracellular calcium waves, based on electrical measurements. With this thesis, it was possible to optimize materials and devices to fabricate electronic devices capable to perform extracellular recording of ultra-weak bio signals.

This work was integrated in the iONE-FP7 Project[1], whose objective was to create a device to repair Spinal Cord Injury. The device is called AMID, an Active Multifunctional Implantable Device. The AMID is fabricated in a biocompatible and biodegradable scaffold. The aim of the research group based at the University of the Algarve is to develop and optimize the individual devices before they are incorporated into the AMID.

Spinal cord injury is a neurodegenerative disease that affects approximately 4 million people worldwide. It is characterized by disconnection of axons, loss of neurons and glia and demyelination associated with a secondary inflammatory degenerative process which leads to variable extension of the lesion area, and consequently, to different functional deficits.

[1] http://ione-fp7.eu/consortium/

Keywords: Implantable device, cell culture, C6 cells, Neuro-2a cells, impedance, drug screening platform, calcium waves.

Results published and submitted for publications

Manuscripts submitted

Henrique L. Gomes, Maria C. R. Medeiros, Ana Mestre, Joana Canudo, Inês M. Araújo, M. L. Cancela, Volker Mailänder, Melanie Dröge, Dago M. de Leeuw, Fabio Biscarini, Leonid Schneider, Paulo R. F. Rocha, "**Electrical Recording And Capacitive Stimulation of Quasi- Periodic Spikes in C6 Glioma Cell Populations"**, Open Biology.

Oral communications

Pedro C. Inacio, Sanaz Asgarifar, **Ana G. Mestre**, Joana Simões Canudo, Inês M. Araújo, M. L. Cancela, Maria do Carmo Medeiros, Fabio Biscarini, Henrique Leonel Gomes, "**Conducting polymer electrodes to measure slow cooperative extracellular signals**", *2015 MRS Fall Meeting Symposium: CC: Organic Bioelectronics—From Biosensing Platforms to Implantable Nanodevices*, 1st-2nd December, Boston (USA) 2015. (Accepted)

P.C. Inácio, **A.G. Mestre**, S. Asgarifar, Carmen S.R. Freire, Inês M. Araújo, M. L. Cancela, M.C. Medeiros, F. Biscarini and Henrique L. Gomes, "**Extracellular recordings from cardiomyocytes using polymer electrodes on nanofibrous bacterial cellulose substrates**", *NANOMED 2015*, 23th-25th November, Manchester (UK) 2015. (Accepted)

Ana G. Mestre Pedro C. Inácio, Inês M. Araújo, M. L. Cancela, Maria C. R. Medeiros, and Henrique L. Gomes, "**Drug screening platform based on extracellular electrical noise measurements**", *NANOMED* 2015, 23th -25th November, Manchester (UK) 2015. (Accepted)

Sanaz Asgarifar , **Ana G. Mestre**, Pedro Inácio, Inês M. Araújo, M. L. Cancela, J. Bragança, Jérôme Borme, George Machado Jr., Fátima Cerqueira, Pedro Alpuim and Henrique L. Gomes, "**Highly sensitive electrochemically gated graphene field-effect**

transistor for extracellular cell signal recording", *NANOMED* 2015, 23th -25th November, Manchester (UK) 2015. (Accepted)

M.C. R. Medeiros, **Ana G. Mestre**, Pedro Inácio, Joana Canudo, Inês M. Araújo, M. L. Cancela, Fabio Biscarini**,** Henrique L. Gomes, **"Ink-jet printed polymer electrodes on bio-cellulose to record extracellular calcium waves produced by neuronal cell populations *in vitro*"**, *E-MRS 2015 Spring Meeting*, 11th-15th May, Lille (France) (2015). **Best paper award of the symposium**

Henrique L. Gomes, Pedro C. Inácio, **Ana G. Mestre**, Joana Canudo, Inês M. Araújo, M. L. Cancela, Maria C. R. Medeiros and Fabio Biscarini, **Semiconducting polymer micro-electrodes and electrical noise based techniques as a tool to probe living cells *in vitro***, MRS, Materials, November 30th-December 5th 2014, Boston, USA.

Ana G. Mestre, **Implantable Organic Nanoelectronics for regenerative medicine**, Departamento de Engenharia Electrónica e Informática, DDEI, 18th December 2014, Faro, Portugal.

Pedro C. Inácio, **Ana G. Mestre**, Joana Canudo, Inês M. Araújo, M. L. Cancela, Luís Alcácer, Maria C. R. Medeiros, Fabio Biscarini and Henrique L. Gomes, **Semi-Conducting Polymer Microelectrodes and Electrical Noise Based Techniques as a Tool to Probe Living Cells *in vitro***, Workshop Nano2014, Academia das Ciências de Lisboa, 10th October 2014 Lisboa, Portugal.

Posters

Ana G. Mestre, Pedro Inácio, Joana S. Canudo, Inês M. Araújo, M. L. Cancela, M. Carmo Medeiros, Henrique L. Gomes, **Active Multifunctional Implantable Device for Regenerative Medicine**, TechDays Conference, 17th-18th September 2015, Aveiro, Portugal.

Ana G. Mestre, Pedro Inácio, Joana S. Canudo, Inês M. Araújo, M. L. Cancela, M. Carmo Medeiros, Henrique L. Gomes, **Electronic Platform for Fundamental**

Neuroscience Research, TechDays Conference, 17th-18th September 2015, Aveiro, Portugal.

Ana G. Mestre, Pedro Inácio, Joana S. Canudo, Inês M. Araújo, M. L. Cancela, M. Carmo Medeiros, Henrique L. Gomes, **Electrical noise as a tool to probe populations of cells *in vitro***, 4th International Conference on Bio-Sensing Technology by Elsevier, 10th-13th May 2015, Lisboa, Portugal.

Joana Canudo, **Ana G. Mestre**, Pedro C. Inácio, Luís Alcácer, Inês M. Araújo, M. L. Cancela, Maria C. R. Medeiros, Fabio Biscarini and Henrique L. Gomes, **Cooperative Bioelectrical Activity On Glioma C6 cells Measured Using Electrical Methods**, 4th International Conference on Bio-Sensing Technology by Elsevier, 10th-13th May 2015, Lisboa, Portugal.

Pedro C. Inácio, **Ana G. Mestre**, Joana Canudo, Luís Alcácer, Inês M. Araújo, M. L. Cancela, Maria C. R. Medeiros, Fabio Biscarini and Henrique L. Gomes**, Ink-jet Printed Polymer Microelectrodes Arrays to Record Electrophisiological Signals of Neuronal Cells *in vitro***, 4th International Conference on Bio-Sensing Technology by Elsevier, 10th-13th May 2015, Lisboa, Portugal.

Ana G. Mestre, Pedro Inácio, Joana S. Canudo, Inês M. Araújo, M. L. Cancela, M. Carmo Medeiros, Henrique L. Gomes, **Presentation of Implantable Organic Nanoelectronics (iONE) Project**, 24º Congresso de comunicações, Centro Cultural de Belém, CCB, Lisboa, 19th-20th November 2014.

Ana G. Mestre, Pedro Inácio, Joana S. Canudo, Inês M. Araújo, M. L. Cancela, M. Carmo Medeiros, Henrique L. Gomes, **Implantable Organic Nanoelectronics (for regenerative medicine)**, Instituto de Telecomunicações, 7th November 2014 Aveiro, Portugal.

Ana G. Mestre, Pedro Inácio, Joana S. Canudo, Inês M. Araújo, M. L. Cancela, M. Carmo Medeiros, Henrique L. Gomes, **Using brain-derived cells to investigate behaviour with chemical and electrical stimulations**, Microbiotech Conference, 6th-8th December 2013, Aveiro, Portugal.

Other dissemination activities

National TV program about science ("*Exame Informática*") see links below.

[1] https://www.youtube.com/watch?v=YhwEOdGtSIg

[2] https://www.facebook.com/video.php?v=834544639922700&set=vb.190354481008389&type=2&theater

[3] Feature article "Um implante pode tratar lesões na medulla espinal?", in the national newspaper "Jornal de Negocios", November (2014).

Index

Index of Figures

Index of Tables

Abbreviations

AC	Alternate Current
AFM	Atomic Force Microscopy
AMID	Active Multifunctional Implantable Device
ASIC	Acid Sensing Ion Channel
ATCC	American Type Culture Collection
C	Capacitance
CNS	Central Nervous System
DC	Direct Current
DMEM	Dulbecco's Modified Eagle Medium
DMP	Dimatix Material Printer
EDTA	Ethylenediamine Tetraacetic Acid
f	Frequency
FBS	Foetal Bovine Serum
FCT	Portuguese Foundation for Science
FET	Field-Effect Transistor
G	Conductance
GABA	Gamma-aminobutyric acid
GluR	Glutamate receptors
ICW	Intercellular Calcium Wave
iONE	Implantable Organic Nanoelectronics
k	Boltzmann Constant
MEA	Micro Electrode Array
MISFET	Metal-Insulator-Semiconductor Field-Effect Transistor
PDCH	Petri dish and Chip Holder
PEDOT	Poly(3,4-ethylenedioxythiophene)
PET	Polyethelene Erephthalate
PNS	Peripheral Nervous System
PSD	Power Spectral Density
PSS	Poly(styrene sulfonic acid)
RC	Resistor-Capacitance
SCI	Spinal Cord Injury
T	Temperature
TTX	Tetrodotoxin
UV	Ultraviolet light

CHAPTER 1

Introduction

1.1 Implantable devices to repair spinal cord injury

The research that constitutes the core subject of this thesis was developed in the context of a project entitled “Implantable Organic Nanoelectronics (i-ONE)”. The iONE Project aims to develop a new tool for treating spinal cord injury (SCI). SCI is a neurodegenerative disease of the central nervous system (CNS) affecting an estimated 2.5 million people worldwide, with more than 130,000 new cases reported each year. SCI has a significant impact on quality of life, life expectancy and represents a significant economic burden, with considerable costs associated with primary care, sometimes resulting in loss of individual income. To date, no treatment for SCI has allowed for a full recovery of lost motility, sensibility and function.

The main rational underpinning the project is to develop a multifunctional device prototyped on the patient, implanted at the SCI site, operated from the outside for the duration of the therapy, that will bio-degrade itself afterwards. The device will allow one to identify a suitable combination of stimuli to evoke and modulate the signal across the region of the injury. It will also enable the controlled delivery of stem cells to the SCI site and stimulate their differentiation into neurons. Its lifetime will be tailored to the duration of the therapy to reduce the risk of a host versus graft immune response. The device must be suitable as to allow neurosurgery to be performed on individuals. The implant is minimally invasive due to its miniaturization, mechanical compliance, conformal adhesion, choice of biodegradable materials and scaffold. Therefor, the envisioned device is a versatile tool for *in-situ* functionality.

The transplantation of stem cells or stem cell-derived progenitors represents a promising therapeutic solution for repairing the damaged nervous system. These cells should be able to develop into functional neurons in order to integrate synaptically into the host brain circuitry. This approach requires implantable multifunctional devices suitable for engrafting neural stem/precursors cells. Devices should have long-term stability associated to high biocompatibility and safety, and reduced risk of a host versus graft immune response. Since stem cell commitment is governed by a combination of top-electro-chemical stimuli, the device should be able to mimic the local microenvironment for stem cell differentiation. This may require a possibility to perform local stimulation with electric fields, local delivery of growth factors, neurotransmitters, and drugs. The integration of highly sensitive transducers in the

implanted device would allow for monitoring the status of the regenerating nerve cells and controlling the auto-immune inflammatory response *in vivo* as demonstrated in Fig.1.1.

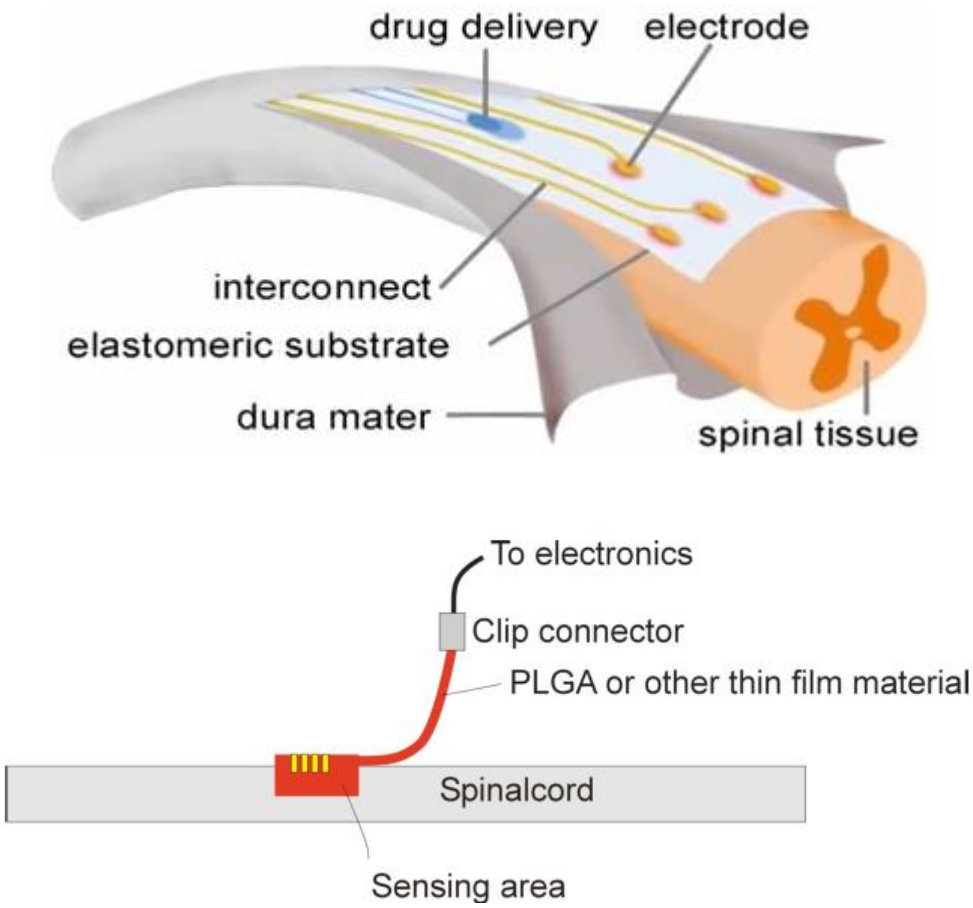

Fig. 1.1 —Schematic demonstration of implantation in the injury place. The implant will be in contact with the spinal cord injury. The sensing area refers to the local where the device will be placed.

Although the device is targeted to the Central Nervous System in terms of design, materials and prototyping approach, the concept can be extended to other organs/tissues and environments, also *in vitro*, where stem cells need to be precisely stimulated. The implanted device will be used for monitoring neuronal transmission at the injury site, thus enabling the follow-up of the therapy in the patient.

In order to promote regeneration, a combination of electrical, chemical and electrochemical stimuli can be used to induce residual plasticity and neural stem cells can be locally delivered and differentiated into neurons. The device provides therapeutic treatment of the inflammation evoked by the spinal cord injury and the following

necrosis.

The implant is bendable in a cylinder like shape. It integrates an array of three type of different devices; as is shown in Fig.1.2 the device is composed of: (i) organic transistors which can supply electric and electro-chemical stimuli to the neurons, (ii) electrodes that can monitor the neurons response; (iii) microfluidics actuated by organic electronics that pump and control the delivery of anti-inflammatory drugs, differentiation and growth factors, and neurotransmitters. Individual devices were studied and optimized at different nodes of the iONE consortium. The role of the Algarve team is to develop a transducer capable of recording signals from the cells and also to stimulate the cells using electrical signals. Part of this work is reported in this thesis.

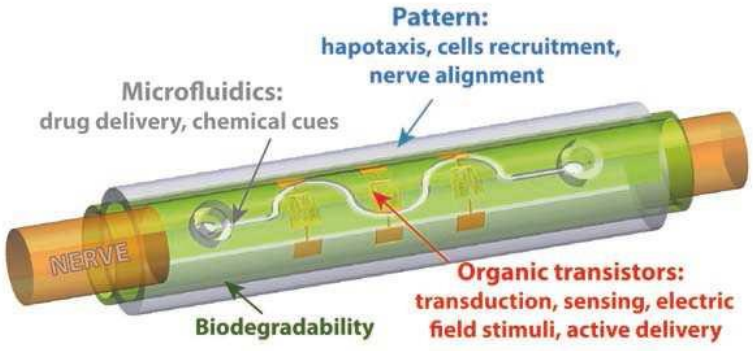

Fig. 1.2 — Prototype of the iONE project device called “AMID” - Active Multifunctional Implantable Device.

During the project the individual devices were optimized and integrated into a final AMID device. Fig. 1.3 shows a photograph of the implantable device.

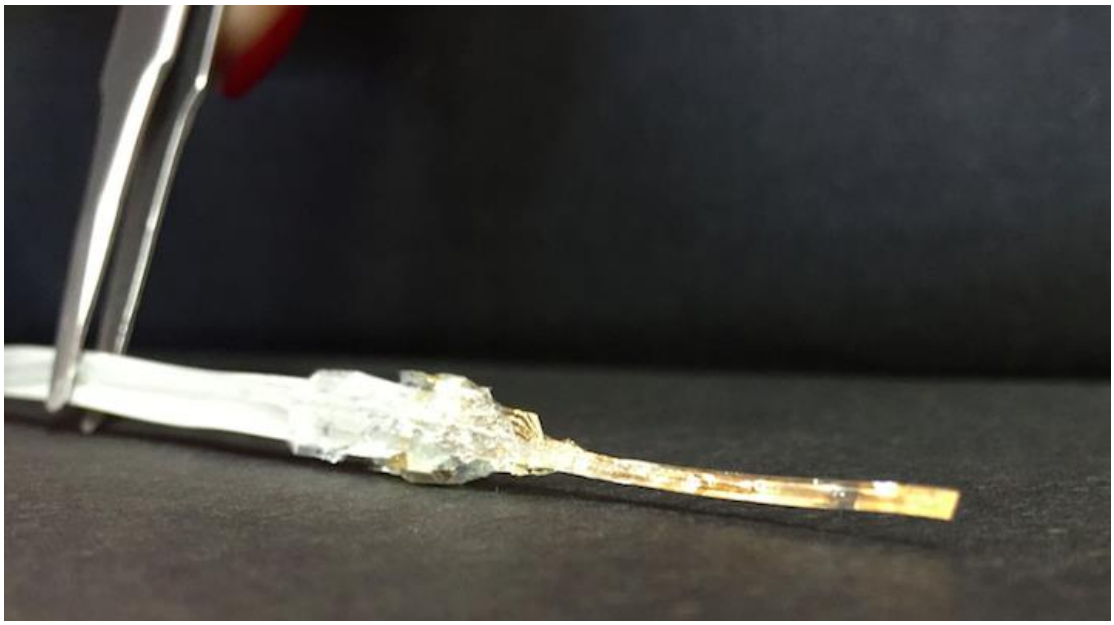

Fig. 1.3 — Photograph of the implantable device produced by the iONE project.

The complexity of both the medical problem and the implant requires the integration of multidisciplinary expertise in bioelectronics, neurology, stem cells, imaging diagnostics, anatomy, experimental neuroimaging, electronic and software engineering,

In this context, the work carried out is relevant to tissue engineering and regenerative medicine. The multi-functionality of the device preludes its potential use in cell therapy and bio-artificial organs due to its capability to monitor/react in real time as is necessary.

1.2 Therapeutical approaches of SCI

There are few examples of SCI therapies based on stem cells that have been approved by regulatory bodies, including the EMA in Europe and FDA in USA. The main difficulty encountered in these therapies concerns the poor control of (1) the cellular sensing and response to the microenvironment, (2) directed cell migration, (3) some key decision-making processes that include proliferation/activation/death, and (4) the precise dynamic control over distribution, level and duration of action. Combining stem cell transplants with the delivery of small molecules such as neurotransmitters and anti-inflammatory drugs to the SCI site coupled with rehabilitation practices for several days is a key technological need that has yet to be met [1], [2].

Traditional management of SCI is about medical, surgical and rehabilitative processes.

In spite of the many evidences provided by animal models that decompression in the local of injury increases functional recovery and minimizes the secondary injury in this disorder, there are some interventions that can be done based on a number of approaches, such as surgical (decompression), pharmacological (administration of methylprednisolone) and electrophysiological (by the stimulation of a specific point).

New approaches for SCI repair that already have been tested include cell therapy with neural stem cells, mesenchymal stem cells, olfactory ensheathing cells, Schwann cells, activated macrophages, embryonic stem cells, but as expected these strategies, whose main features and respective outcomes are detailed in Table 1.1, minimized but did not repair the injury [3].

Table 1.1 – SCI repair involving cellular therapy.

System	Outcome
Neural stem cells	Able to differentiate into neurons, oligodendrocytes and astrocytes; concerning SCI, they are used to replace the loss of tissue and to foster trophic support for the survival neural tissue. It was tested *in vitro* and *in vivo* (adult rats) [4], [5].
Mesenchymal stem cells	Used for regenerative applications, these cells are easy to isolate and expand; they also have anti-inflammatory and anti-immunosuppressant effect and do not form tumours. They are derived from the bone marrow. In traumatic SCI models experimental studies led to some motor improvements. The cells were injected into or next to the SCI site, but they can be delivered intrathecally or intravenously [6]–[12].
Olfactory ensheathing cells	Play an important role in the lifelong neural regeneration capacity of olfactory neurons in adult rats. They can create a permissive microenvironment for axonal regeneration across the injury site in humans [13]–[15].
Schwann cells	Promote axonal regeneration and myelination in adult rat thoracic spinal cord [16], [17].
Activated macrophages	Capable of producing growth factors and scavenging neurotoxins such as excessive quantities of glutamate. Sufficiently activated macrophages can contribute positively to the homeostasis of the central nervous system. In preclinical studies, recovery of hind-limb function has been reported after transection and transplantation of macrophages that had been previously activated with PNS tissue [18]–[20].
Embryonic stem cells	Indefinite ability of self-renew and they can differentiate into cells from all three germ layers. In order to obtain a desirable cell population, in vitro was performed pre-differentiation mouse ES cells in neurons and olidendrocytes. Both resulted in remyelination and functional recovery in contusion SCI animals [21]–[23].

Besides cells therapy, both molecular therapy and combinatorial therapies were tested. Tissue engineering holds great promise for SCI because of the possibility of tissue regeneration (including bone, cartilage, neurons and muscle). Needing to include a specific set of characteristics, a scaffold created for tissue engineering must (i) be biocompatible; (ii) have desirable physical characteristics (high porosity, large surface area), (iii) be biodegradable and (iv) have desirable surface properties (to deliver drugs) [3], [24], [25]**.** Tissue engineering strategies to repair SCI have been energetically tested in the past years and are summarized in Table 1.2.

Table 1.2 – SCI repair strategies. For each, the system applied, the SCI model (rodent) and the respective results are shown.

System	Outcome
Implantation of synthetic non-degradable hydrogel PHPMA (poly-(2-hydroxypropyl)-methacrylamine) modified with the amino acid sequence RGD	Functional recovery; regeneration of sensory axons; decrease in scar tissue formation; little invasion of regenerating axons into the channels; studied in chronic transection SCI model [26][26]–[29].
Implantation of synthetic polymers with the biomaterial PEG (polyethylene glycol)	Repairs cell membrane breaches; decrease excitotoxicity; inhibit the production of free radicals; decrease lesion volume; attenuate in macrophage response; improved motor outcomes [30], [31].
Implantation of PEG-PLA (PEG-poly-lactic acid) hydrogel containing NT3	Improves BBB score and ladder walker performance; increases the number of axons [32].
Combination of NSCs and synthetic PLGA (poly-lactic-co-glycolic acid) scaffolds with aligned porosity	Reduces scar formation; improves functional recovery [33].
Synthetic matrix composed by peptide amphiphile (PA)	Improves motor function; reduces astrogliosis; decreases cell death; promotes regeneration of ascending and descending track axons through the local of injury; descending track axons through the lesion site [34].
Collagen	Increases the number of axons either when used alone in combination with NT3 or even when used to fill PHEMA-MMA and chitosan tubes; implantation in SCI rodents to fill the gap in transection models of SCI [27], [35]–[37].
The use of Matrigel and contains several bioactive molecules, such as laminin, fibronectin, and proteoglycans, with laminin predominating	NSCs differentiation into neurons and oligodendrocytes; increases sensory axonal regeneration; cell infiltration through the gel; increases angiogenesis and SCs survival; facilitates intralesional axon growth; promotes functional recovery; injected in a contusion rat model of SCI [38], [39].
Fibrin, is probably the most extensively used hydrogel in SCI.	Releases NT3 after degradation by invading cells; increases nervous cells infiltration; diminished the glial scar. Moreover, the use of fibrin in combination with cAMP and pre-differentiated NSCs resulted in extensive axonal regeneration into the injury site of fully transected rats; improved functional recovery after 6 weeks [40]–[44].
Agarose and Alginate	Decrease of the lesion volume; Macrophages invasion; proteoglycans content; oxidative stress; production of BDNF encapsulated in alginate micro-capsules, could be delivery to the spinal cord without the need for immunosuppression; growth of regenerating axons; improved the function of affected limbs; injected in a hemisection rat model of SCI [45], [46].
3D biodegradables structures based on rapid prototyped starch poly-caprolactone scaffolds	Improvements in distance traveled and rearing activity in rats with SCI [3].

1.3 Objective

The aim of this thesis was to study the cellular behaviour of neural cells in electronic devices by creating a bridge between electronics and biology. With this purpose in mind, neural cells, Neuro2a cells (neuroblastoma) and C6 cells (glioma) that were cultured in a diversity of electronic devices comprising different characteristics, such as the material of the substrate (Polyethelene Erephthalate (PET), SiO_2, Titanium, Bacterial Cellulose) and the material of the electrodes (Gold and poly (3,4-ethylenedioxythiophene) polystyrene sulfonate (PEDOT:PSS)). For the iONE-FP7 Project, our group in University of Algarve aimed at optimising the AMID by measuring the neural cells in the devices provided by the partners in the iONE –FP7 consortium.

Within this framework, the role of the UAlg team was to develop an electronic transducer to monitor living cells and their response to a number of electrical and chemical stimuli in real time. These cell cultures are adherent and were used as prototype cells to test the transducer and the electrical addressing techniques. These cells were electrically and chemically stimulated and were monitored using a set of electrical techniques, which includes low-frequency impedance and electrical noise. The major achievements of this work are outlined below.

This thesis is organized as follows: Chapter 1 contains the introductory remarks explaining the context of the work and reviewing the state-of-art; Chapter 2 outlines the experimental techniques and describes in details the cell cultures utilised; in turn, Chapter 3 focus on the use of small-signal impedance methods to gain information about cell adhesion and viability; Chapter 4 describes the electrical measuring method used to detect cell electrical activity and presents the possibility of using electrical noise as a drug-screening platform; Chapter 5 follows by presenting the observation of intercellular calcium waves electrically; finally, the major conclusions of this thesis are summarized in Chapter 6, that also contains a list of recommendations for further work and research.

CHAPTER 2

Methods and Techniques

This chapter describes the experimental methods, the cultured cells and the geometry of the electrodes arrays used. The electronic instrumentation used to record extracellular signals is also outlined.

2.1 Device layout and structure

This section gives an overview of the experimental set-up developed for performing *in-vitro* measurements. The main components of the *in-vitro* experiments are: (i) the device; (ii) the "device holder", which allows making electrical connections between the device and the instrumentation, and confines the cell medium on the active surface of the sensor device; (iii) the incubator and finally, (iv) the amplifier and the spectrum analyzer. The devices used for measurements consisted of simple microelectrode arrays fabricated using gold or ink-jet printed polymers on glass or on bacterial cellulose. Some of the designs used are shown in Fig. 2.1. Typical device dimensions and surface morphologies are shown in Fig. 2.2.

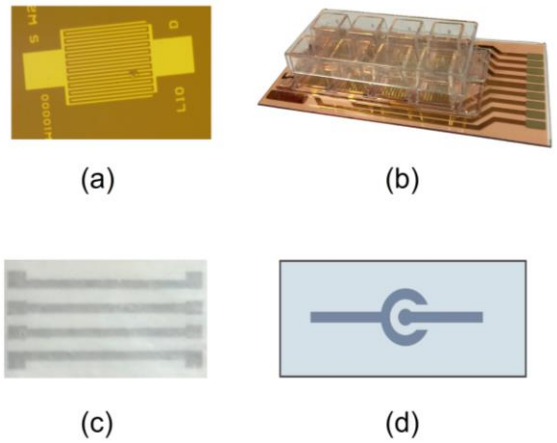

Fig. 2.1 — Electrode designs used in this thesis. (a) Gold microelectrode arrays on top of thermal oxidized silicon wafers, (b) Commercial available electrodes on plastic substrates (PET), (c) Electrode geometries using printed polymers on bacterial cellulose substrate, (d) Electrode geometries using printed polymers on glass substrate.

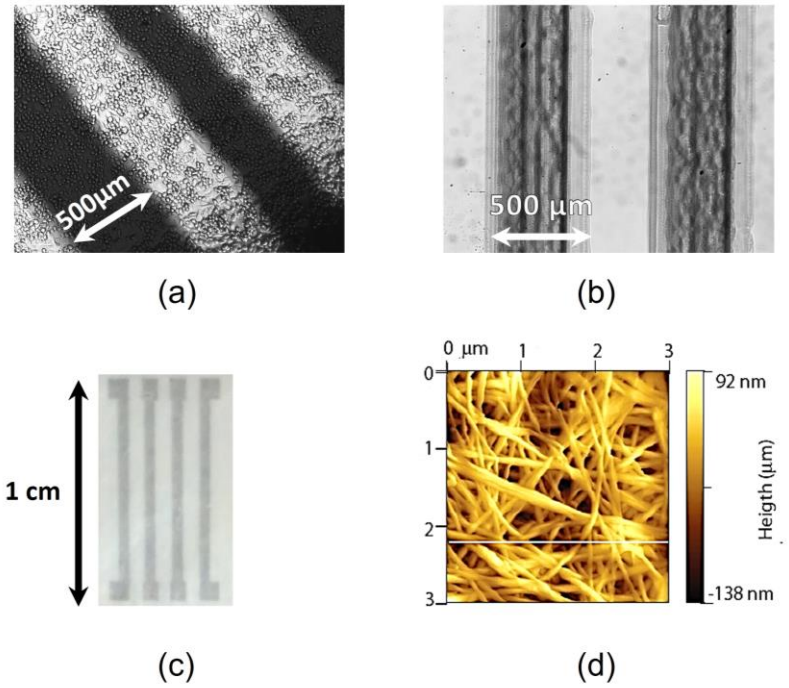

Fig. 2.2 — Electrode dimensions and surface morphologies. (a) Photograph of the C6 cells on top of glass substrates with gold electrodes. The darker regions are the gold regions (transparent substrate) (b) Photograph of the ink-jet printed PEDOT fingers on glass, (c) Typical bacterial cellulose substrate with ink-jet printed PEDOT electrodes and (d) Atomic Force Microscopy (AFM) photograph of the bacterial cellulose nanofibrous structure.

Gold interdigitated electrodes on the top of oxidized silicon wafers were explored as transducers to electrically stimulate the cells. Each wafer has 4 devices with different inter-electrode distances. A typical layout is shown in Fig. 2.3. The silicon wafer on the top surface is thermally oxidized (SiO_2). The bidirectional transducer (Fig.2.3) is an interdigitated microelectrode array (Philips Innovation Services, Eindhoven, The Netherlands) fabricated on thermally oxidised Si wafers 150mm in diameter. The oxide is 200nm thick and can be used to couple alternative current (AC) signals to the cells. The Au electrode arrays were 10000µm long and separated apart by 20µm.

The thin insulating top layer can be used as a capacitive layer to electrically stimulate the cells. The device resembles a metal-insulator-semiconductor (MIS) structure. Voltage pulses can be applied to the gate voltage and capacitive coupled into the electrolyte solution and to the cells.

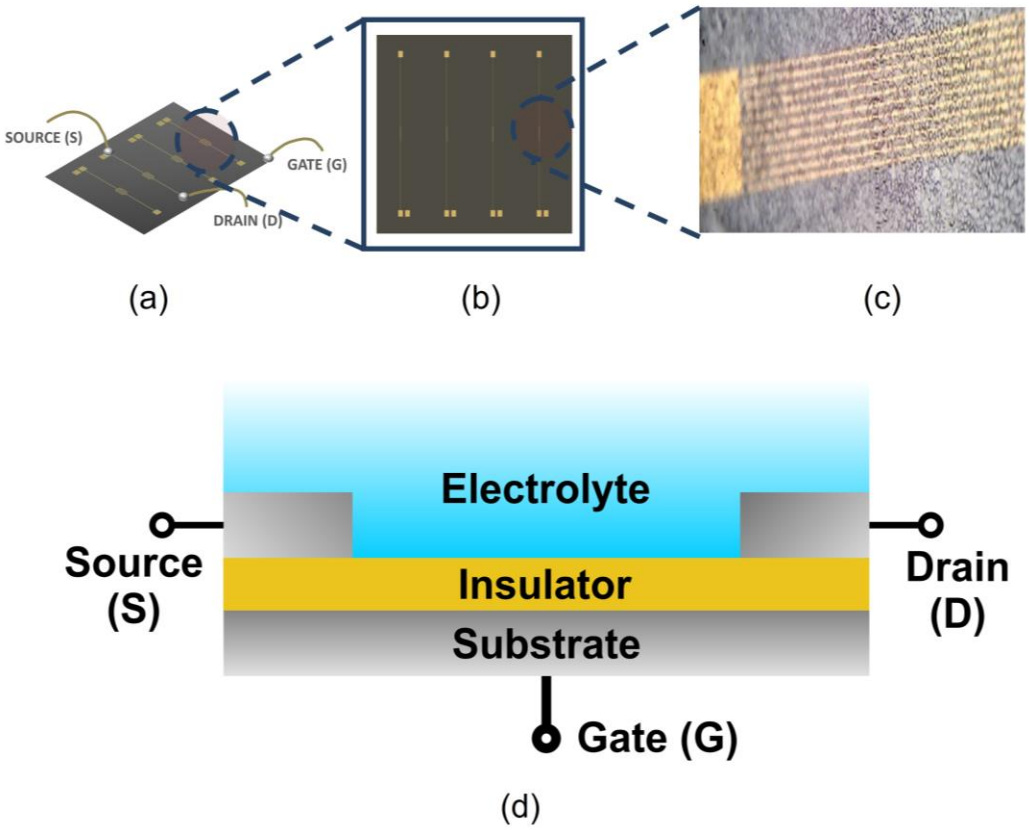

Fig. 2.3 — (a) and (b) Individual silicon wafer with 4 microelectrode arrays, (c) Detailed view of the gold electrode fingers and (d) Cross sectional view of the device structure with the electrolyte solution, showing the three terminals, source, drain and gate.

Moreover, commercially available electrodes with built-in vessels to hold the cell cultures were also used. These devices were supplied by the company IBIDI (http://ibidi.com/). These electrodes were made of semi transparent gold on a plastic substrate (PET). A detailed view of the electrodes is shown in Fig. 2.4.

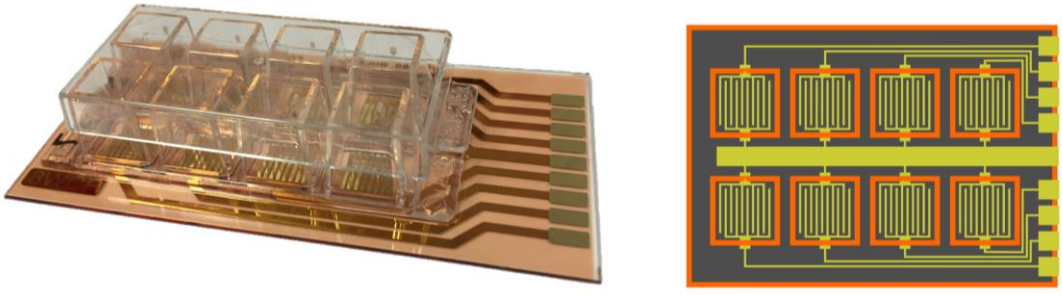

Fig. 2.4 — Gold microelectrodes on plastic provided by IBIDI (http://ibidi.com/).

2.2 Device holders

The device holders are supports designed to hold a variety of sensing devices and can be plugged into several measuring systems. Furthermore, they allow keeping cell cultures alive over extended periods of time (weeks) due to a sufficiently large cell reservoir (>200μL), and since they were designed in transparent materials, visual inspection is also possible.

The Petri dish and Chip Holder (PDCH) (see Fig. 2.5 developed by UAlg) is the proposed device to perform assays of cells culture *in vitro*. The assembled prototype was fabricated using transparent extruded acrylic. It makes use of a standard commercial available Petri dish (4cm in diameter). The sensing devices were glued onto commercial available glass slides. Electrical contacts were sealed from electrolyte using commercial available biocompatible o-rings. The Petri dish has the capacity of 2mL of cell culture medium. The entire system can be used in inverted microscopes. Fig. 2.5 shows the different steps to assemble the chip holder. Fig. 2.6 shows a typical sensing device using bacterial cellulose as a substrate mounted in a Petri dish. Bacterial cellulose is a biomaterial with physical and mechanical properties of interest that can be used both as a substrate and in addressing the use of such membranes for drug loading and controlled release.

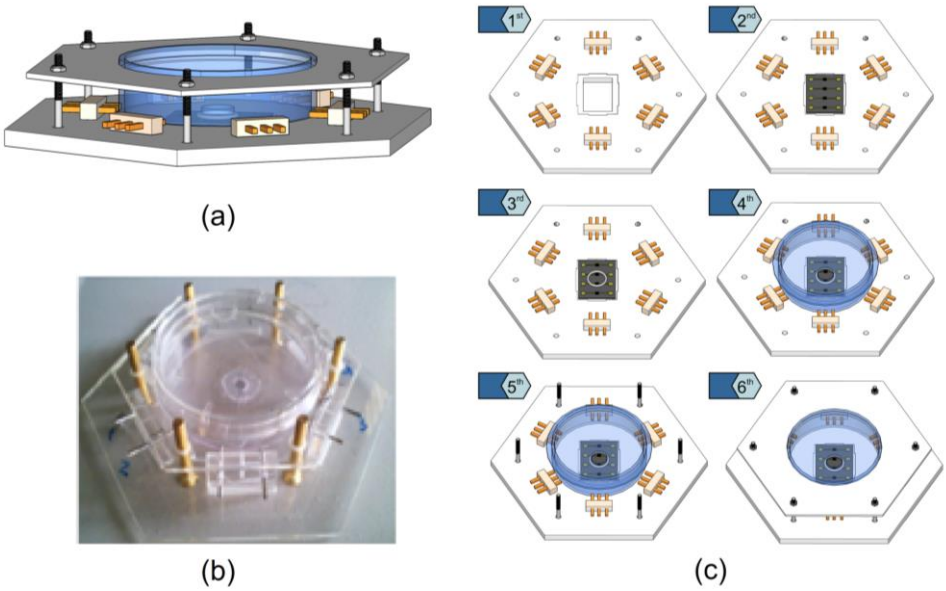

Fig. 2.5 — Schematics of a Petri dish and Chip Holder (PDCH). (a) Schematic representation of the PDCH, (b) Photograph of a device holder mounted and (c) Schematics representation.

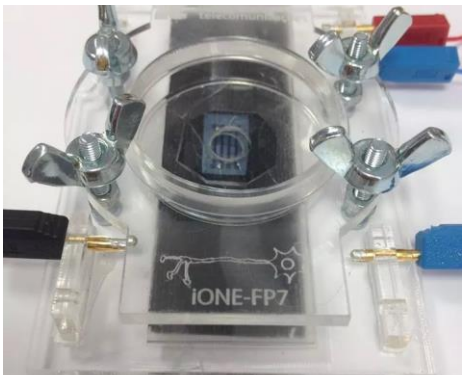

Fig. 2.6 — Typical sensing device using bacterial cellulose as a substrate mounted in a Petri dish.

Cellulose substrates were produced by a bacteria from the *Gluconacetobacter genus* that produces an extremely variety of bacterial cellulose, in the form of a highly swollen membrane, with around 99% water, on the culture medium surface [47].

2.3 Polymer electrodes

Ink-jet printing is a method of deposition of functional materials. Some examples of functional materials that can be ink-jet printed include metal inks, conductive and semi-conductive polymers, proteins and nanoparticles.

Inkjet printing is a cost-effective and flexible method used in several research areas such as chemical, mechanical, optical researches and in a wide range of applications like electronics, optoelectronics and displays [48].

Polymer electrodes, poly (3,4-ethylenedioxythiophene) polystyrene sulfonate (PEDOT:PSS), were fabricated by inkjet-printing. Printing was performed using a Fujifilm Dimatix Material Printer (DMP) 2831, with a DMC-11610 cartridge. This cartridge contains 16 nozzles, which generates 10ρl drops of ink. For all electrodes, an aqueous dispersion of PEDOT:PSS was employed, which after solvent drying and thermal annealing, formed into a continuous and transparent conducting film. Before filling the cartridge, PEDOT:PSS based ink was subjected to a ultrasonic bath for 15 min.

For glass devices during printing, substrates were kept at a constant temperature of 55˚C to help fast solvent evaporation and bacterial cellulose devices are kept at room temperature. For substrates, glass and bacterial cellulose, electrodes were fabricated with 8 printed layers with a drop spacing of 30µm. In order to minimize ink spreading

on the substrate, a waiting period of 30 minutes between each layer was observed. After printing, samples were annealed on a hot plate at 60˚C for 8h. After annealing, the devices were immersed in an ethyleneglycol solution. Finally, the devices were dried in a vacuum oven at 60˚C for 12h and bacterial cellulose substrate samples were annealed on a hot plate at 40ºC for 8h.

An approach using PEDOT:PSS electrodes on both substrates that are particularly suited to measure cell populations that engage into cooperative activity was also used. The relevant characteristics of this kind of device are their flexibility and biocompatibility.

2.4 Electronic acquisition system

The electrical activity of the cells was recorded using the experimental set-up described in Fig. 2.7. This set-up is comprised of an Agilent 35670A Dynamic Signal Analyzer, a low-noise current pre-amplifier Stanford Research SR 570 or, alternatively, a low noise voltage amplifier the SRS 560. Electrical excitation was applied using a pulse generator 32220A. The sensing devices were kept inside the incubator. The entire system was operating inside a large iron box with an electrical ground to shield external sources of electrical noise and interference (see Fig. 2.7).

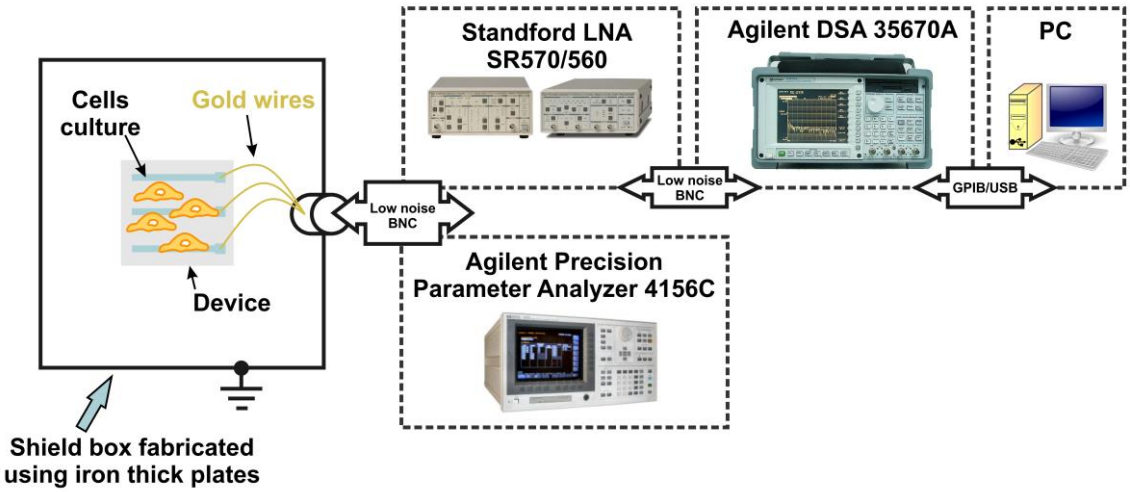

Fig. 2.7 — Experimental setup. Equipment used to record bioelectrical signals. The equipment is inside an iron-based Faraday cage in order to remove interferences.

2.5 Electrode dimensions

The sensing devices use two parallel electrodes of depth, *D*, separated by a channel length *L* and width, *W*. The coplanar electrode design is show in Fig. 2.8. The figure also represents the labels corresponding to the electrode dimensions. Standard electrode dimensions are shown in table 2.1.

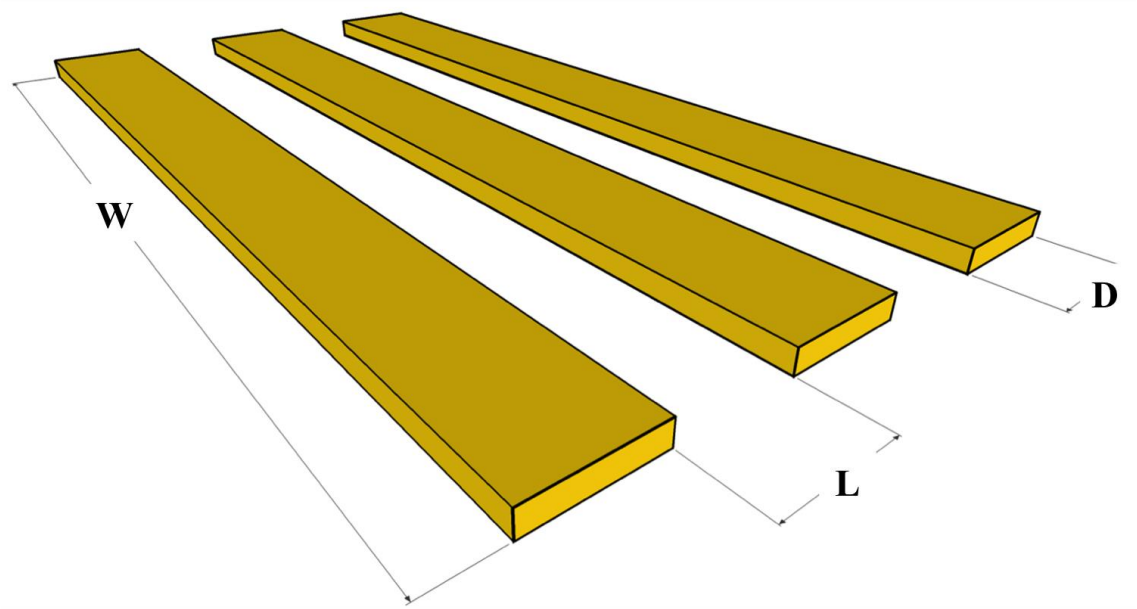

Fig. 2.8 — Electrode design showing the depth (D), length (L) and width (W).

Table 2.1 — Standard device dimensions used.

Device	Width (µm)	D_{GAP} (µm)	Length (µm)
IBIDI – 8WCP (GOLD/P3MT electrodes)	8	640	215
IBIDI – 8WCP PET (GOLD/P3MT electrodes)	3520	100	325
PHILIPS – 4 MISFET (GOLD/P3MT electrodes)	1000	5	10
Glass + PLGA (PEDOT electrodes)	7000	500	600
Bacterial cellulose + PLGA (PEDOT electrodes)	7000	500	800
Gold electrodes (Glass + TiO_2)	3670	340	610
Gold electrodes (Bio-cellulose)	4000	325	180

2.6 Sterilization and coating procedures

Prior to cell deposition the devices were sterilized (utilising an ultraviolet light) and coated with poly-L-lysine 0.01% provided by Sigma-Aldrich in order to promote cell adhesion. The surface of the device was washed with sterilized water and after that it was covered with poly-L-lysine for 5 minutes. Finally, the poly-L-lysine was removed and washed again with sterilized water, and the devices were ready to use with cells after 2h.

2.7 Cell cultures

For *in vitro* measurement protocols several different cell types were tested, namely: (i) Neuro-2a (*Mus musculus*, Mouse neuroblastoma) and (ii) C6 cells, *Rattus norvegicus*, (Rat). Cell viability and pH kinetics assay were performed on 96 well plates. The cells were grown in culture plates and then detached, diluted in culture medium to yield cell suspensions with a known cell density and transferred to the sensing devices. An aliquot of 350μL of the cell suspension (concentration≈$5.1x10^6$ cells/mL) was transferred to the well of the sensing device and cells were allowed to settle onto the device for 2h before any measurements were performed.

In case a chemical stimulation is required, a cell culture medium with a defined concentration of the chemical was prepared. This solution was then used to replace the cell culture medium.

The pH on supernatants was measured with Lab850 pH-meter (Schott Instruments). Cell numbers and viability were assessed using a Neubauer chamber-based trypan blue live/dead exclusion assay. The device loaded with the cells was then incubated in a cell incubator (HERACell®150) that was kept clean. The incubator kept the cells under a humidified atmosphere at 37ºC with 5% CO_2. Half of the medium was changed every 4-5 hours.

Regarding the experiments three different types of mediums were used: (i) Krebs medium, (ii) F-12K Nut Mix medium, and (iii) DMEM (1x). Krebs Medium composed by 132mM NaCl, 4mM KCl, 1,4mM MgCl2, 6mM Glucose and 10mM Hepes-Na at a pH of 7.4. The F-12K Nut Mix (1x) composed by Nutrient Mixture supplemented with 15% horse serum, 2.5% foetal bovine serum (FBS) and 1% penicillin and streptomycin

was used for C6 cells. And finally, DMEM (1x), 10% foetal bovine serum (FBS) and 1% of penicillin and streptomycin was used for Neuro-2a cell cultures.

2.7.1 Neuro-2a cells

Neuro-2a cells (American Type Culture Collection, ATCC) were cultured in DMEM (1x), 10% foetal bovine serum (FBS) and 1% of penicillin and streptomycin. The cells were maintained in a humidified atmosphere at 5% of CO_2 and 37ºC. The medium was changed every two days. In Fig. 2.9 is possible to see Neuro-2a cells in culture.

Neuro-2a cells are derived from mouses and the morphology of this kind of cells is neuronal. The cell type is neuroblast. Neuro-2a cells are adherent cells capable of producing action potentials [49].

We applied 5 million cells/mL of Neuro-2a cells on the device and incubated them at 37ºC and 5% CO_2 for 2hours previous to the experiments.

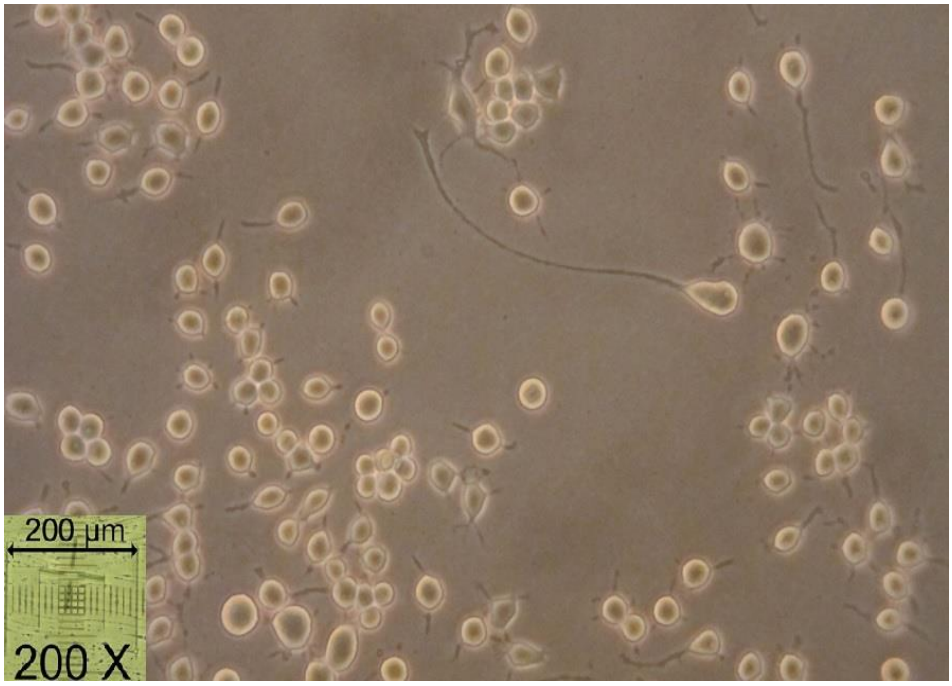

Fig. 2.9 — Neuro2a cells in culture. Scale bar: 200 µm.

2.7.2 C6 cells

Rat glioma C6 cells (American Type Culture Collection, ATCC) were cultured in 15% F-12K Nut Mix (1x) supplemented with 15% of foetal horse serum, 2.5% of foetal bovine serum and 1% of penicillin and streptomycin (see Fig.2.10). C6 cells have a fibroblast-like morphology and they grow as an adherent monolayer. Besides having sodium, calcium and potassium channels [50], Glial cells have ionotropic glutamate receptors (iGluRs), ionotropic GABA receptors ($GABA_a$ and $GABA_c$), glucocorticoid and glycine receptors [51], [52], which allow us to stimulate them chemically. In this case, the concentration used was approximately $5.1x10^6$ cells/mL.

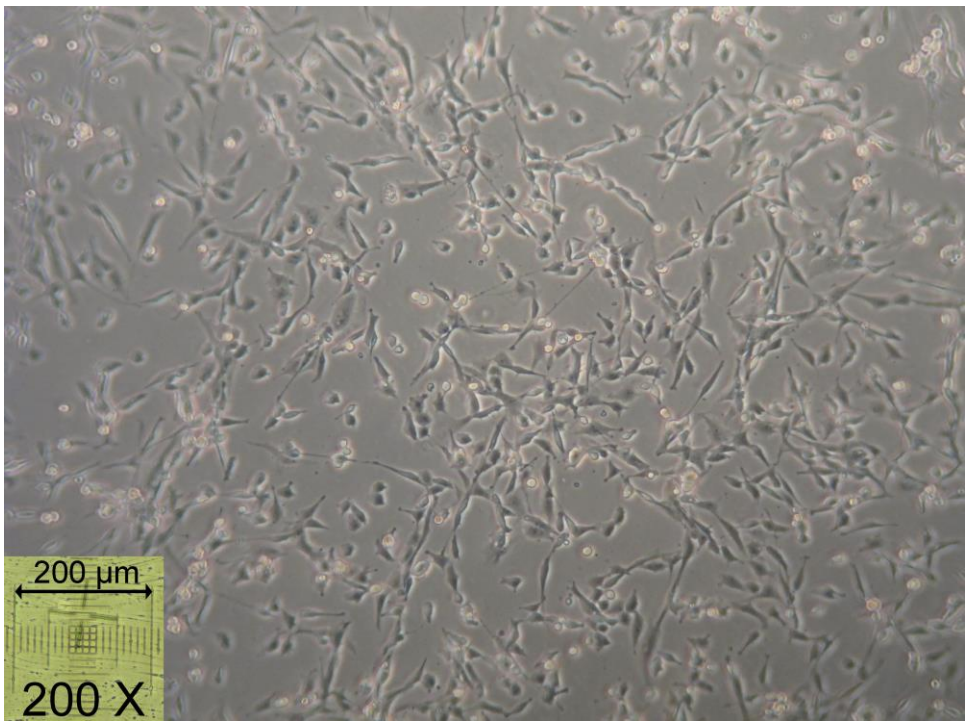

Fig. 2.10 — C6 cells in culture. Scale bar: 200 µm.

CHAPTER 3

Cell adhesion and device stability

This chapter presents a study of the impedance of the electrodes used to record extracellular signals. The dependence of the impedance on the (i) electrode material, (ii) cell culture medium, (iii) cell density, (iv) medium acidity and (v) temporal drifts are addressed in this chapter. Drifts on impedance are important because they have an impact on the electrical coupling between the cells and the sensing electrodes, as well as the coupling between the electrodes and the sensing instrumentation. Understanding the physical origin of these drifts is crucial to obtaining high quality extracellular recordings. The ability of the impedance methods to detect small chemical variations at the cell/electrode interface is also discussed.

3.1 Introduction

When the electrodes are immersed in an electrolyte solution this system physically behaves as a two-layer system. One of the layers is comprised of a charged interfacial region established on both electrode surfaces known as Helmholtz or Stern layer. A schematic representation of this layer is show in Fig. 3.1.

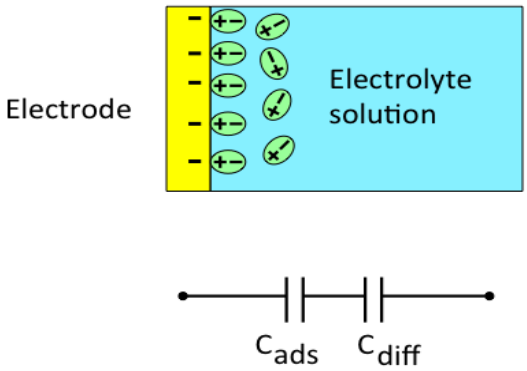

Fig. 3.1 — Schematic representation of the Helmholtz layer established at the eletcrode/electrolyte interface. This charged layer has a capacitance and is convenientely described by a capacitor. A more accurate representation may use two capacitors arranged in series, one to take into account the layer near to the surface (C_{ads}) in series with a more extended layer $C_{diff.}$

The Helmholtz layer is arranged in series the bulk electrolyte solution connecting the two electrodes. The two layers are connected in series. A convenient way to interpret the overall system's electrical properties is to use an equivalent circuit network. Each layer is described by a parallel RC network. One RC takes into account the high interfacial capacitance (C_{DL}) and, usually, also a high interfacial resistance (R_{DL}). The bulk electrolyte is better described by a low capacitance (C_B) in parallel with a resistance (R_B) that accounts for the bulk conductivity of the solution. Both interfacial regions are physically identical; therefore, only one RC circuit is required to describe them. The RC circuits describing the interface and the bulk layer are effectively in series and provide an electrical equivalent for the two-layer system as schematically depicted in Fig.3.2 [53].

This network has a frequency response as shown in Fig. 3.2 where the capacitance (C) and loss is represented as a function of the frequency. The loss is defined as $1/(\omega R_P)$, where R is the resistance and $\omega=2\pi f$, and f the frequency of the test signal.

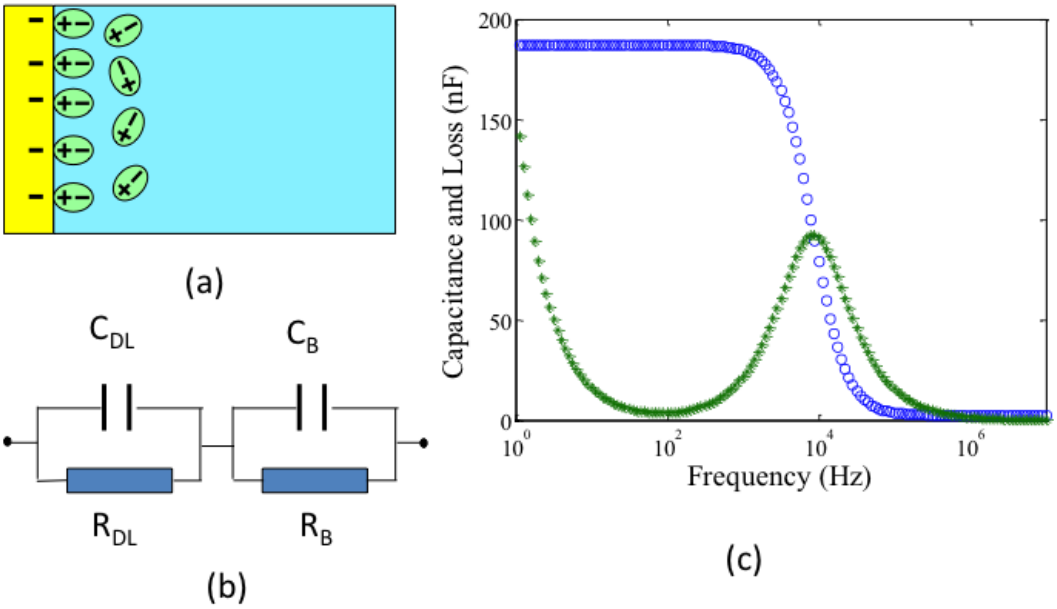

Fig. 3.2 — The Helmholtz capacitive layer established in the metal/electrolyte interface can be electrically simulated by a double RC circuit show on (b). The ideal frequency response of this circuit is shown on (c) for the capacitance and loss (1/(Rω).

The values of the capacitance and resistance of the double-layer Helmholtz region control the amplitude of the noise generated by the electrodes. Furthermore, these impedance parameters also control the electrical coupling to the pre-amplifier. It may limit the available bandwidth [54].

The electrode impedance magnitude as well as the frequency dependence is contingent to the activity of the cells and their adhesion to the microelectrodes. Also, the cells have their own impedance characteristics mainly determined by their structure. Changes in the cell have an effect on their impedance, providing important information about their viability and physiology. Impedance biosensors have been used for screening cells, monitoring cell proliferation, morphology, motility, and, more recently, some reports include also sensors for pharmaceutical screening, environmental monitoring and toxin detection [53], [54].

The measuring method is based on the disturbance of the electrode impedance by the cells. The cellular membrane is an electrically insulating structure. It basically behaves as a capacitor. When the membrane covers the electrodes, it blocks the high frequency electric field. This is schematically represented in Fig. 3.3. If there are gap regions between the cells, the high frequency electric field lines flow easily through the electrolyte medium and the low-frequency ones through the membranes. The system is particularly conductive when the signal is relatively high in frequency (above a few kHz). When the cells coat the electrodes, the electric field has to pass through the

cellular membrane (highly resistive and capacitive). The membrane is transparent for high frequency signals, which is not the case for low frequency signals. The frequency response of the electrodes depends on the electrode cell coverage and on the shape of the cells. For this reason the impedance measurements are often used to monitor cell adhesion [53].

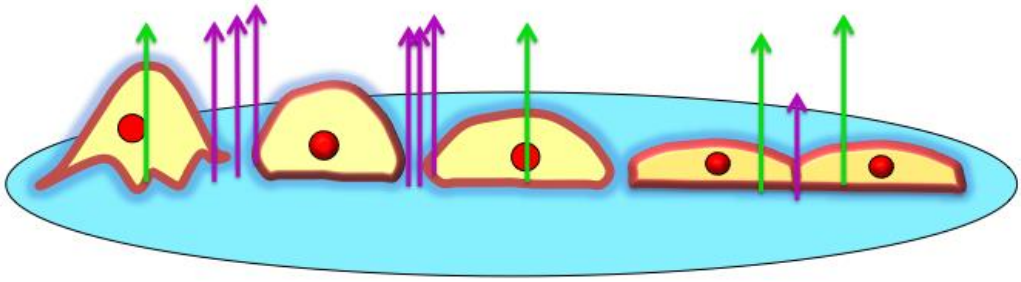

Fig. 3.3 — Schematic representation of how the electric field lines flow amid the gap junctions between cells. This is valid for ac signals in the frequency range of a few kHz. The pink lines represent the high frequency signals flowing trough the gap junctions. The green lines represent the low frequency field flowing trough the membrane.

3.2 Experimental

Fig. 3.4 shows a schematic representation of the electrodes coated with cells and the connections to the measuring instrumentation. It also shows the equivalent circuit network that conveniently describes the frequency dependence of the electrodes immersed in an electrolyte solution. The electrodes are directly connected to the impedance analyser, the Fluke PM6306. Small-signal impedance measurements were carried out in the frequency range 60Hz to 1MHz. The amplitude of the test signal is 50mV.

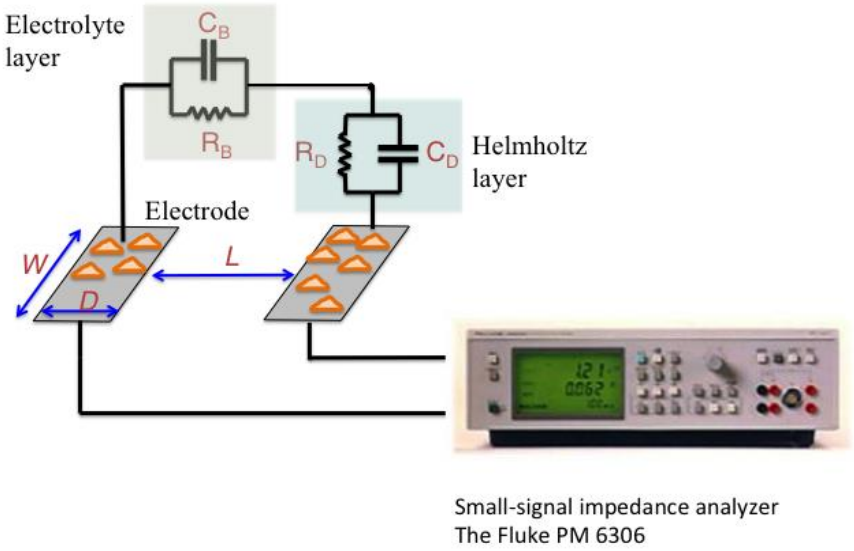

Fig. 3.4 — Schematic diagram of the sensing device structure and connections to the impedance analyzer. The labels of the electrode's physical dimensions are also show. Devices' dimensions are described in Table 2.1 (chapter 2).

3.3 Results

In this section is present the experimental behavior of the sensing electrodes utilized. The individual circuit parameters, namely the capacitance and the resistance of the sensing electrodes are extracted. This extraction can be done by measuring the capacitance (C) and the conductance (G), according to the frequency. A typical frequency behavior is demonstrated in Fig. 3.5 where the capacitance as a function of frequency (f) is presented for three sensing electrodes: (i) gold electrode on silicon, (ii) printed PEDOT:PSS on glass and (iii) printed PEDOT:PSS on bacterial cellulose. The capacitance of the gold electrode shows dispersion centered on 200kHz, a phenomenon typical of the Maxwell–Wagner relaxation process observed in two-layer dielectric structures. The frequency (f_R) of this relaxation is related with individual circuit components by $f_R=1/2\pi(C_B+C_{DL})$. The continuous red line on Fig. 3.5 represents the fitting to the capacitance curve using the double RC network shown in Fig. 3.2.

For PEDOT:PSS electrodes, the Maxwell–Wagner relaxation is not in our frequency observation window. This is because the electrodes are separated by a large inter-electrode distance (L=600μm). As a consequence, the R_B is relatively high and moves the Maxwell–Wagner relaxation frequency below 10Hz, which stands outside of our frequency observation window. However, if the capacitance curve is extrapolated to the

low-frequency region (as shown in Fig. 3.5), it is possible to observe that the capacitance at low frequencies is higher for polymer-based electrodes.

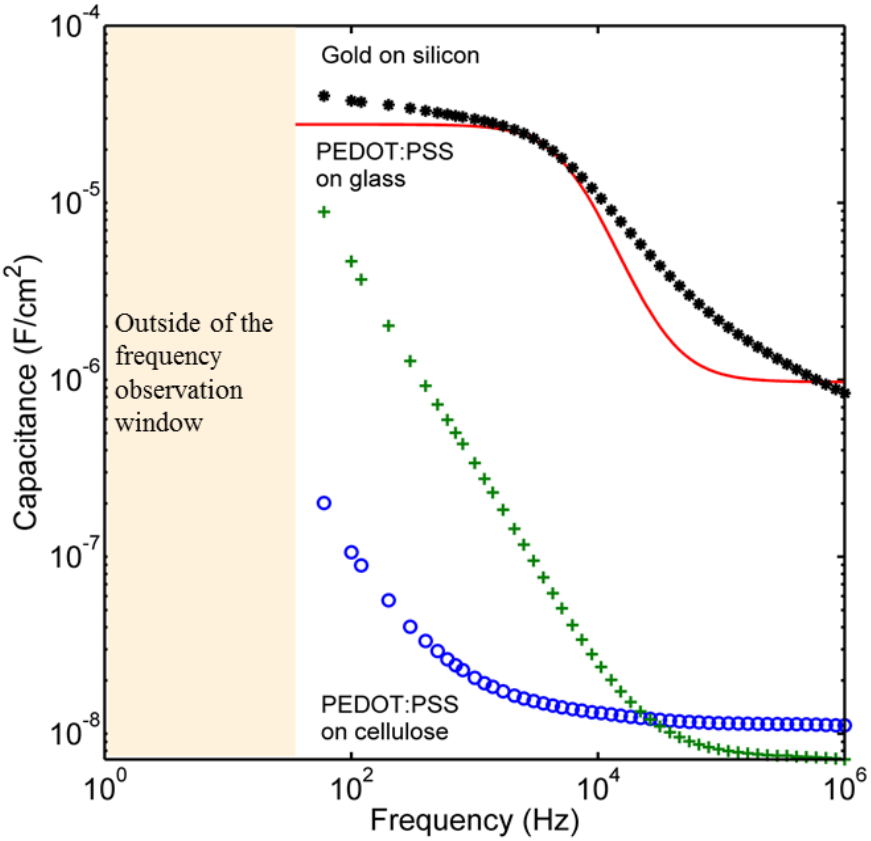

Fig. 3.5 — The frequency dependence of the capacitance for the different electrodes used. The continuous blue and green line is extrapolations to low frequencies, whereas the red line represents the simulation to a perfect Maxwell-Wagner relaxation using a double-RC network.

3.3.1 The drift of the impedance with time

The impedance of the electrodes immersed in a cell culture medium varies with time. This drift is particularly pronounced in the low frequency region (below the Maxwell-Wagner relaxation frequency). Fig. 3.6 shows how the capacitance and the loss curves evolve with time. The capacitance increases with time and the loss peak shifts to low frequencies. The inset shows the time evolution of the capacitance and loss measured at 100Hz. The increase is very rapid in the first 3-5 hours and then increases slowly over time. In summary, the capacitance of the electrodes increases roughly 47% in the first 5 hours. The resistance of the electrodes (measured at 100Hz) also decreases with time. The change in resistance is also pronounced and higher than 60% [54], [55].

To summarize, in the first 5 hours after the addition of the cell suspension to the electrodes, the electrode undergoes a noticeable change in the impedance. The capacitance increases roughly 50% and the resistance decreases more than 60%. The loss peak moves to lower frequencies and increases in magnitude. The frequency shift in the loss is due to the coating of the electrodes by the cells. As aforementioned, the adhesion of the cells to the electrodes blocks the AC conduction between the two electrodes. Although this is an interfacial effect, it appears as a change in the bulk electrolyte conduction.

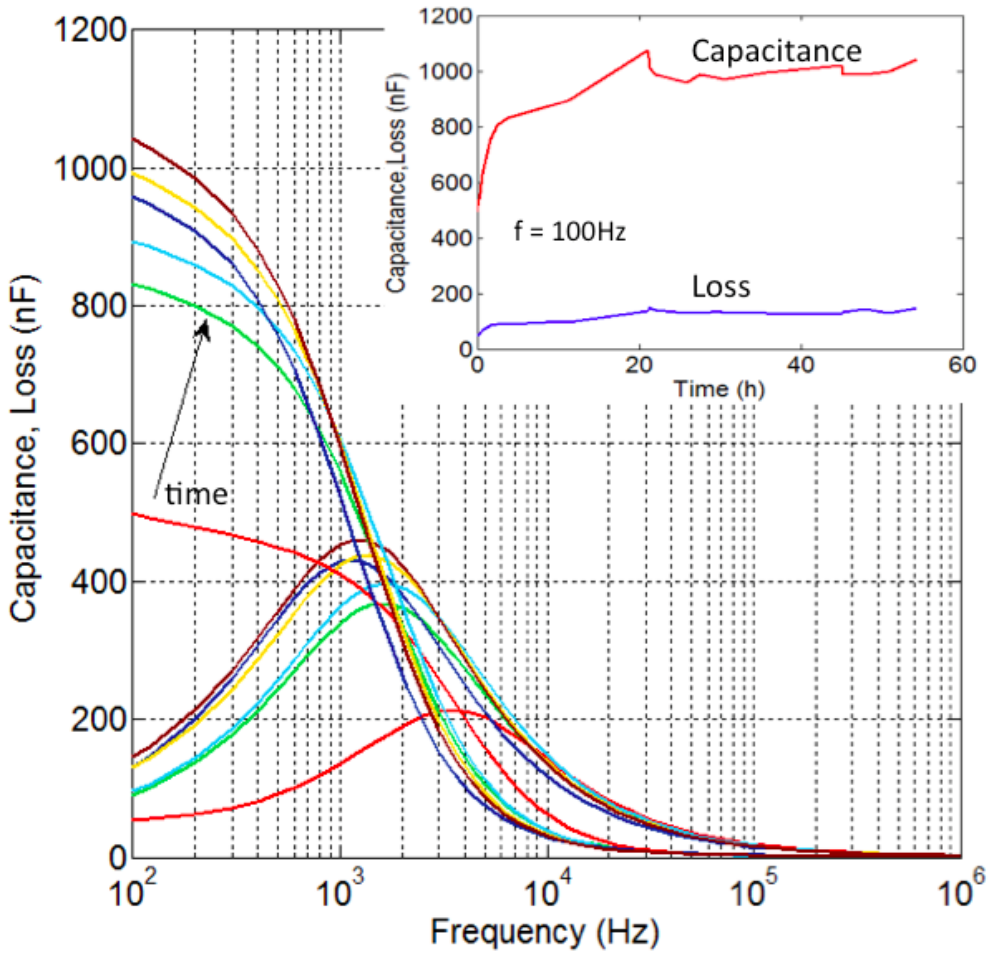

Fig. 3.6 — Temporal evolution of the frequency dependence and time dependence of the capacitance and loss.

While the cell adhesion process readily explains the frequency shift in the loss, the low frequency increase in capacitance is more difficult to account for. It is not clear if this drift is caused by the presence of living cells on top of the electrode or by the deposition

of chemical substances present in the solution. In order to gain insight into the factors causing this drift in the impedance, the time dependence of the impedance was monitored as function of the time. This monitoring was carried out on electrodes immersed only in the cell culture mediums and for electrodes coated with different densities of cells. Two different cell culture mediums were tested, the Krebs medium and the F-12K medium. The F-12K medium was extensively used in C6 cells experiments. The chemical composition of both mediums is complex and it is described in chapter 2.

Fig. 3.7 shows the frequency dependence of the capacitance and loss for the Krebs medium and for the F-12K medium. Although both electrodes are physically identical, the magnitude and the frequency response of the impedance is very different. The first thing to note is that the electrode immersed in the Krebs medium has a Maxwell-Wagner relaxation (f<10 kHz) lower than in the F-12K medium (f>10 kHz). This is because the Krebs medium is more resistive. However, in spite of the lower electrical conductivity, the Krebs medium has a smaller interfacial resistance than the F-12K medium. The loss [1/(Rω)] at 100Hz is 5 times higher in the Krebs medium. The low-frequency capacitance of the Krebs medium is also enormous, 4 times higher than the capacitance of the F-12K medium. In summary, a gold electrode has overall impedance 4 times lower in a Krebs medium than in a F-12K medium. This confirms the role of the interfacial chemistry in controlling the impedance of the electrode.

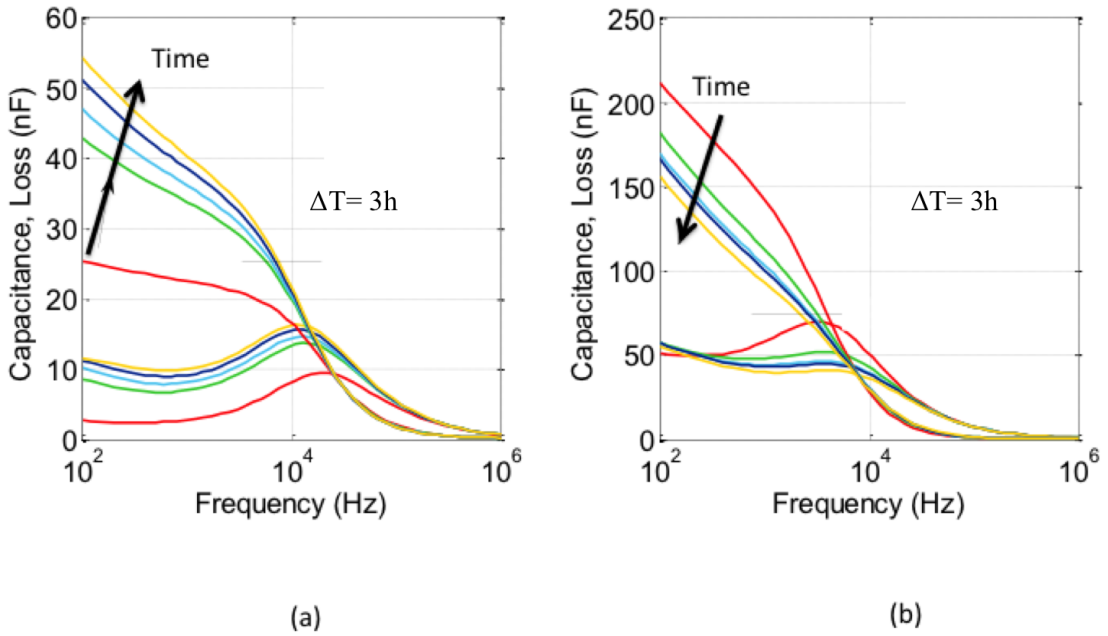

Fig. 3.7 — The time dependence of the impedance spectrum for two cell culture mediums: (a) for the Krebs medium and (b) for the F-12K medium.

The time evolution and time dependence of the impedance was also studied and compared for the two types of mediums. Fig. 3.8a and Fig. 3.9a show the time dependence of the impedance spectrum for both mediums. Fig. 3.8b and Fig. 3.9b shows the time evolution of a single frequency of 100Hz. The two mediums behave in opposite ways. While for the Krebs medium the capacitance decreases over time and in the frequency, for the F-12K medium the capacitance increases over time and in the frequency. The relative changes in the capacitance are high and reach roughly 50% of the total impedance. These changes occur in a time scale of 5 hours.

As is to be expected, the shift in frequency of the loss peak is very small because there are no cells on top of the electrodes. However, over time, the peak also increases in magnitude in the presence of cells. This behaviour is common in both types of mediums.

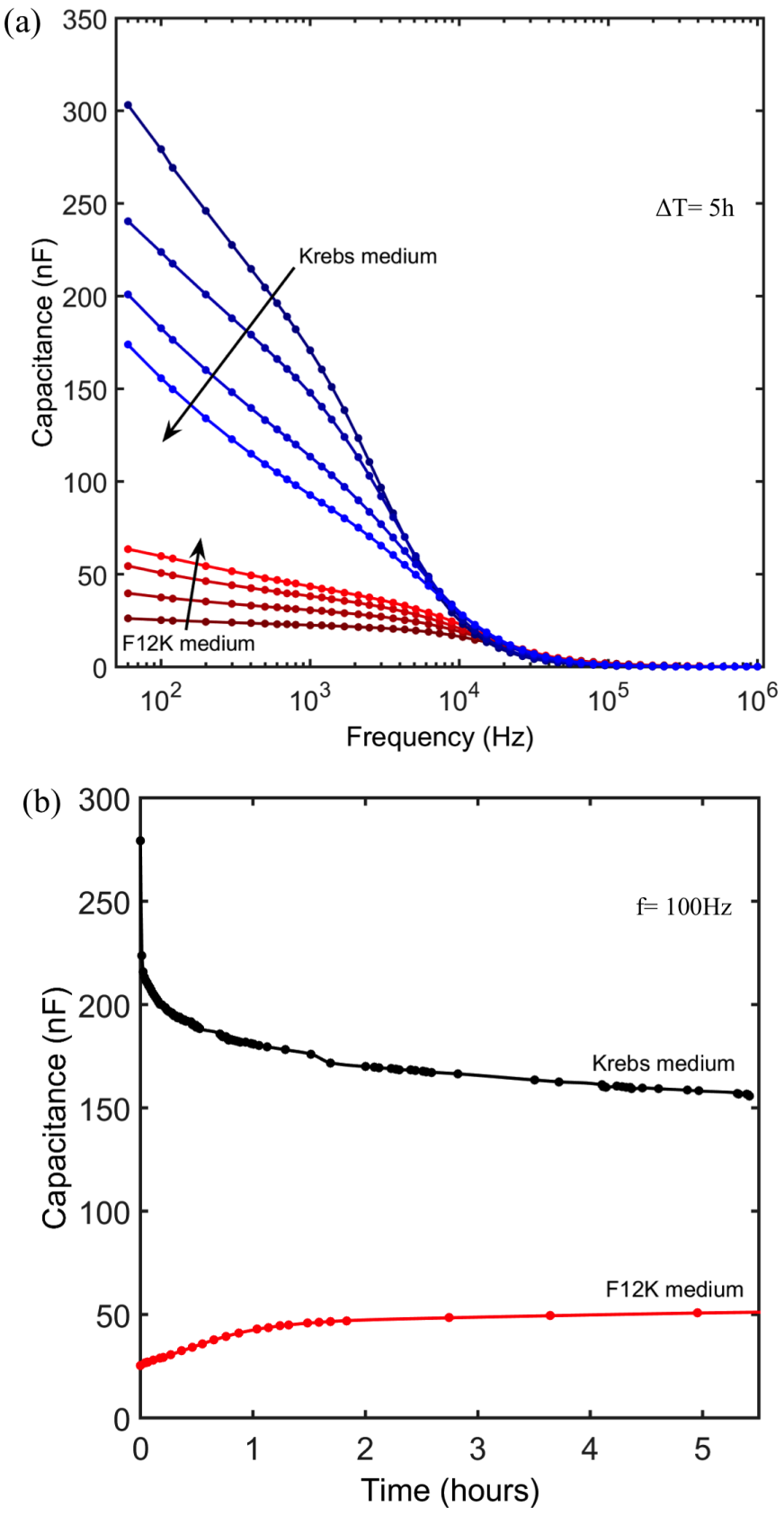

Fig. 3.8 — Time dependence and time evolution of the capacitance spectrum for Krebs medium and F-12K medium. (a) Time dependence for both mediums. (b) The capacitance evolution measured at a single frequency of 100Hz.

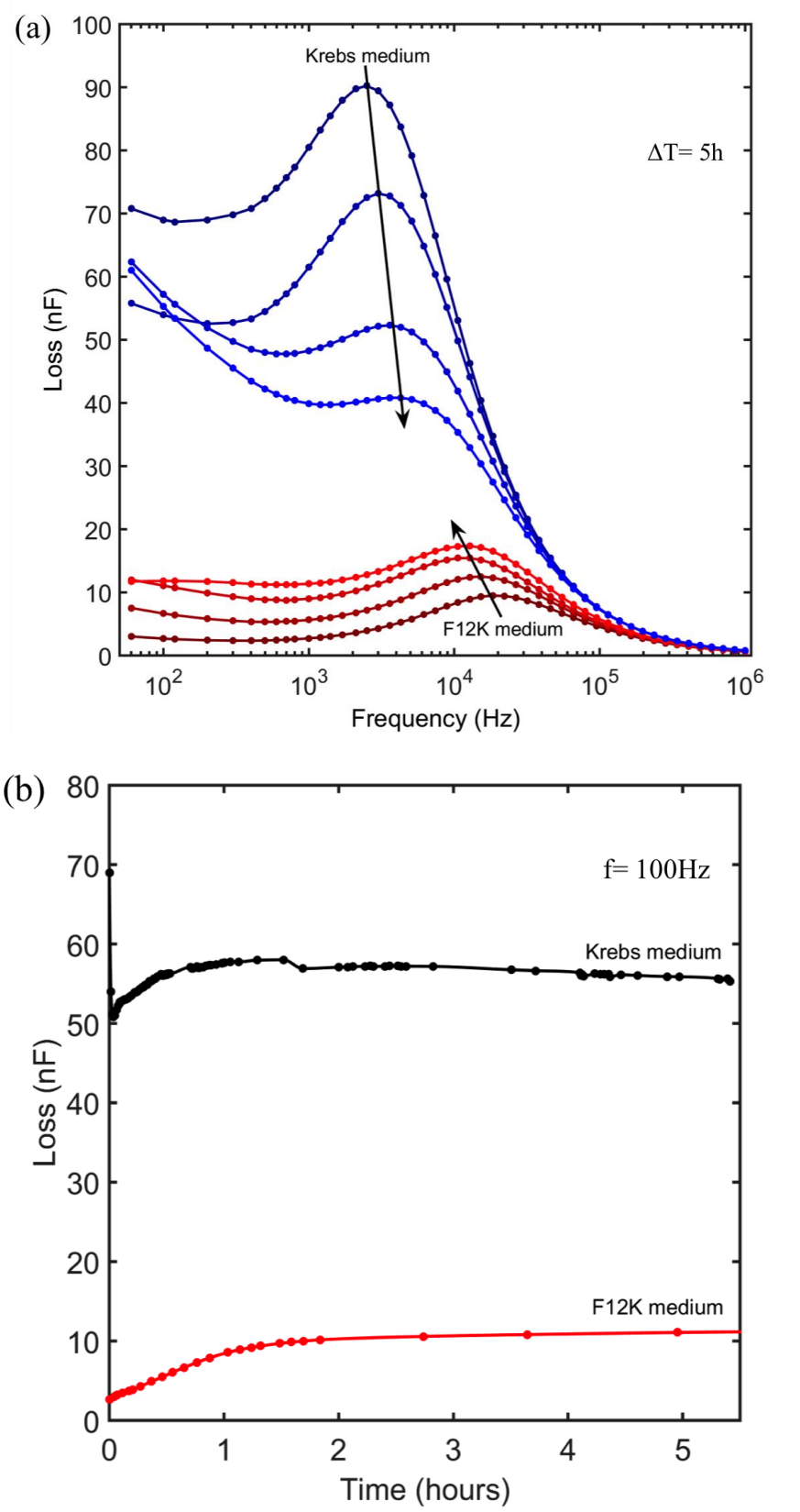

Fig. 3.9 — The time dependence and time evolution of the loss peak for a gold electrode immersed in two types of mediums: Krebs medium and F-12K medium. (a) Time dependence for both mediums. (b) The capacitance evolution measured at a single frequency of 100Hz.

3.3.2 The effect of the cell density on the impedance

The impedance is very sensitive to the cell density. Fig. 3.10 shows the capacitance and the loss curves for two cell densities in gold microelectrode arrays on a silicon substrate (Philips device). The higher the cell concentration, the lower the Maxwell-Wagner relaxation frequency. More interesting are the differences in the frequency dependence. The electrode with a low cell density approaches the ideal frequency response as shown in Fig. 3.2. This means the capacitance is relatively flat for low frequencies. For the system with a high density of cells, the capacitance is strongly frequency dependent and the low frequency capacitance plateau is not observed.

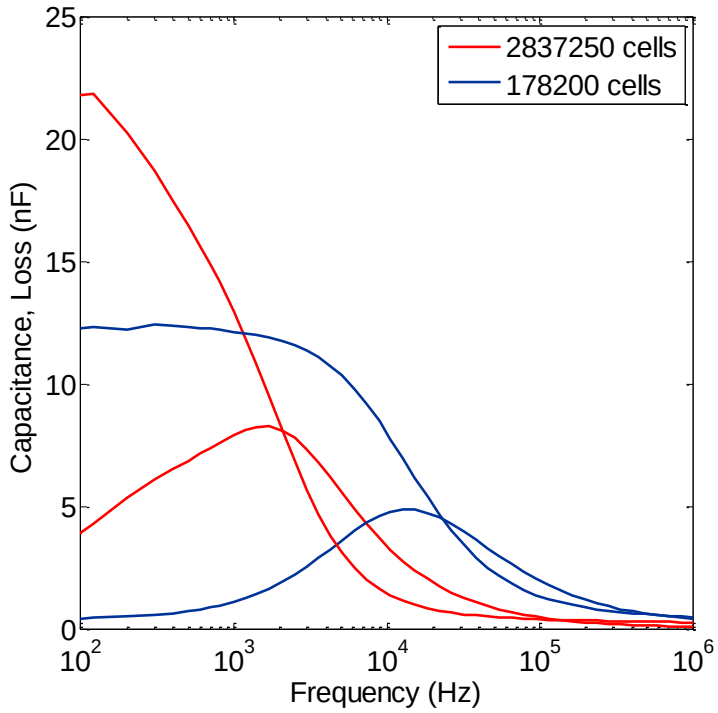

Fig. 3.10 — The frequency response of the capacitance and loss for two cell densities. The electrodes used are inter-digitated gold electrodes on silicon (Philips device) coated with C6 cells.

The cell density has also a marked influence on the time dependence of the impedance. Fig. 3.11 compares the time evolution of the impedance curves, for a lower and for a higher cell density. The surge in capacitance over time is very pronounced when the electrode is coated with a high cell density.

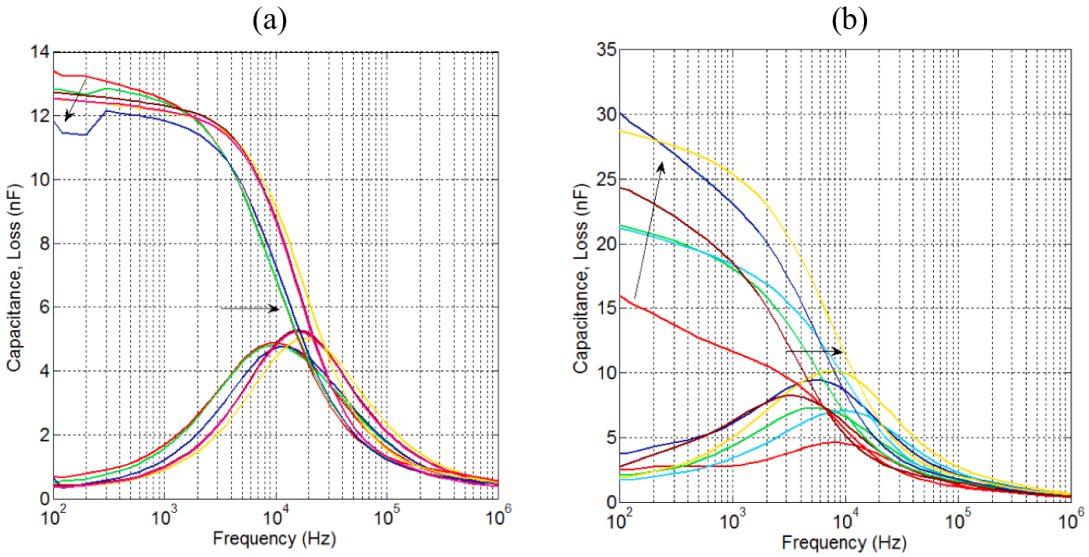

Fig. 3.11 — The effect of cell density on the time dependence of the impedance (a) 178200 cells and (b) 1803375 cells. The impedance was measured on a Philips device using C6 cells.

3.3.3 Changes on the impedance upon chemical stimulation

The impedance of the sensing electrodes was periodically monitored during all the experiments. During a particular experiment using C6 cells, fluctuations in the impedance were observed. A correlation between the impedance data and the electrical current data had shown that the fluctuations in impedance occurred approximately at the onset of the electrical activity. This correlation is shown in Fig. 3.12. After 5 hours from the start of the experiment, fluctuations in the loss are observed and spikes were also visible on the time trace records of the current. This electrical activity will be discussed in further detail in chapter 5.

This observation suggests that the impedance is sensitive to chemical changes occurring near the surface of the electrode. A literature search provided evidence that glioma cells release lactic acid, which interact with the substrate. This is a strategy used by the cells to proliferate and move [56].

To gain insight into the sensitivity of the impedance to chemicals, experiments were conducted where lactic acid was intentionally added to the cell culture medium.

Fig. 3.13 shows the time dependence of the capacitance and the loss measured at the frequency of 100Hz after 2 hours. 8.3mM of lactic acid solutions were added to the cells culture medium. Changes were observed both in the loss as well as in the capacitance. This finding is highly relevant because it shows that by monitoring the impedance it is

possible to detect chemical changes caused by the cells. Therefore, it is also possible to argue that these chemical induced changes can be related to the biological activity.

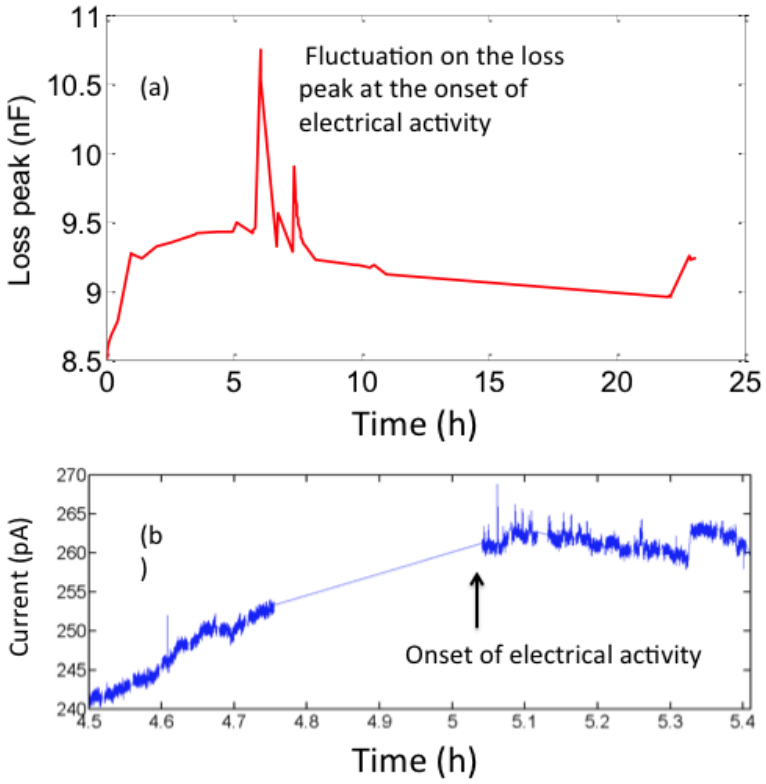

Fig. 3.12 — Correlation between impedance and electrical noise data. (a) Fluctuations in the impedance occur simultaneously at the onset of electrical activity. These data were recorded using C6 cells.

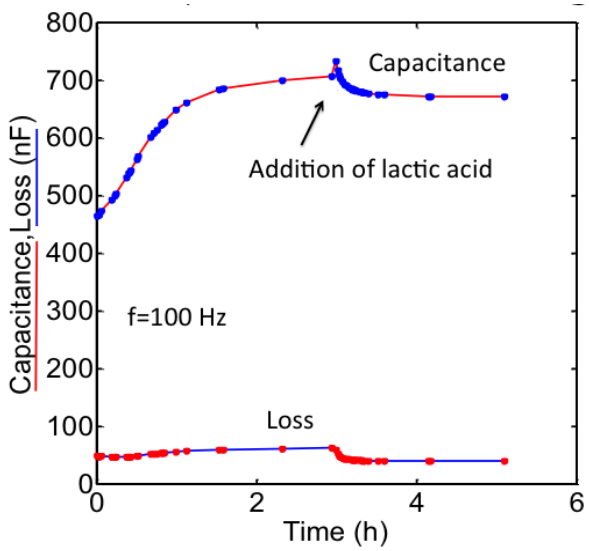

Fig. 3.13 — The effect on the capacitance and loss with a 8.3mM solution of lactic acid added to the cell culture medium.

3.4 Conclusions

In this chapter small-signal impedance measures were used to study the impedance of different sensing electrodes. It was shown that polymer based electrodes have a lower impedance than metallic gold electrodes. The reason for that may reside in the roughness of the surface. Polymers are very rough materials and this increases the total active area contributing to an overall decrease of the impedance. However, it should not be excluded that the complex chemistry of the top surface also plays a role in this low impedance. In reality, the bulk electrode properties do not have significant influence on the impedance of the sensing electrode, which is essentially related to the electrochemistry occurring in the electrode/cell culture interface.

Highly relevant in the context of this thesis is the observation that the impedance of the electrode varies constantly over time, particularly in the first 5 hours after the addition of the cell culture medium to the electrodes. Several types of changes were observed. While some changes were clearly triggered to the presence of the cells, others were related with the cell culture medium.

The shift of the impedance curves to low frequencies has been reported in the literature. It is now well established that this is caused by the coating of the electrodes by the cells. So far, to the best of our knowledge the constant increase of the capacitance and the decrease in the low frequency resistance have not been reported. These drifts are related to the presence of the cell culture medium. Different cell culture mediums cause different and even opposite drifts. While the Krebs medium causes a decrease in capacitance, the F12-K medium causes an increase in the low-frequency capacitance over time. The changes in the impedance are relevant because they modify the noise generated by the electrode and the coupling to the electronic instrumentation. Further experiments are necessary to elucidate which are the chemical species responsible for these impedance drifts present in the cell culture medium. These results also show that the impedance is sensitive enough to detect small chemical changes induced by the cells. Lactic acid seems to be the substance detected, just before the onset of electrical cell activity. This finding is highly relevant for the development of future methods for looking at chemical induced changes caused by cells. The impedance is a non-invasive method simpler than electrochemical methods such as cycled voltammetry.

CHAPTER 4

Drug-Screening Platform

This chapter explores the possibility of using non-invasive electrical techniques to fabricate a drug-screening platform using cells as sensors. The experiments described in this section present a look into how the electrical noise of the interface between cells and electrodes is affected when the cells are exposed to chemical substances.

4.1 Introduction

Electrogenic cells do not always generate clear individual signals; normal metabolic activity generates a low-frequency electrical noise. Cells are noise-generating machines. The cell bioelectrical noise should reflect cellular activity and the viability of the cells. When it is possible to distinguish these cell-induced fluctuations from the intrinsic background noise, we are provided with a tool to monitor a cell's population non-invasively in real time. This technique requires electrodes with intrinsic low-noise. The magnitude of this noise must be below the electrical noise generated by the recording amplifiers. Therefore, in practical terms, our detection limit will be only limited by the recording electronics and not by the sensor [57], [58]. During this thesis an intensive effort was devoted to fabricating and optimizing electrodes with an extremely low noise. In order to achieve that, we have to understand what controls the electrical noise of electrodes immersed in an electrolyte solution. This will be addressed in the following section. Since we use a commercial available amplifier, the noise of the amplifier itself will not be discussed here. We assume the noise is in accordance with the specifications provided by the manufacturer.

4.2 Electrode noise analysis

In this section we studied how the noise of the sensing electrodes depends on the electrode impedance parameters and the measuring bandwidth.

The input circuit to the current amplifier is the double RC network presented in chapter 3. This can be converted into a simpler parallel RC circuit as shown in the inset of Fig. 4.1. This circuit generates input noise, but also changes the overall system performance of the current amplifier. These effects are related with the impedance matching between the sensing electrodes and the amplifier and, thus, will not be addressed here.

The equivalent impedance of the input circuit, Z_M is defined as

(Eq. 4.1)

$$Z_M = R_P + \frac{1}{j\omega C_P}$$

Here the resistive component R_P is given by

(Eq. 4.2)

$$R_P = \frac{(R_{DL} + R_B)^2 + \omega^2 R_{DL}^2 R_B^2 (C_{DL} + C_B)^2}{R_{DL} + R_B + \omega^2 R_{DL} R_B \left(R_{DL} C_{DL}^2 + R_B C_B^2\right)}$$

It has been shown by several authors that only the resistive part contributes to the noise. The power spectral density (PSD) of the current noise generated by Z_M is S_M (f) and can be calculated as:

(Eq. 4.3)

$$S_M(f) = \frac{4kT}{Re\{Z_M(f)\}} \left[\frac{A^2}{H_z}\right]$$

Where k is the Boltzmann constant and T the temperature in Kelvins.

If we use the experimental resistance values based on the frequency, we can estimate the noise of our sensing electrodes using the Eq.4.1. Fig. 4.1 shows the noise spectral density using experimental impedance data for gold and for PEDOT:PSS electrodes. While for gold electrodes the noise increases with the frequency, for PEDOT:PSS electrodes it is almost flat. This difference in behaviour between the two electrode materials is a consequence of the frequency dependence of the resistance.

There are a number of important conclusions that can be extracted from the Eq. 4.3. In order to minimize the noise of the electrodes, interfacial Helmholtz layers with a high resistance and a high capacitance are desirable. The lower the frequency the lower the noise. One has to keep in mind this is true when the electrical fluctuations are measured as an electrical current. To take advantage of this low electrode noise we must carry the measurements at a low frequency. It is also important to point out that this analysis is not valid when the measurements are made in voltage mode. Signals measured as a voltage are affected by a noise that is directly proportional to the resistance. This is according to the equation:

(Eq. 4.4)

$$v_n = \sqrt{4 k_B T R \Delta f}$$

k_B is Boltzmann's constant (joules per Kelvin) and T is the resistor's absolute temperature in Kelvin.

Measuring electrical current is highly advantageous (comparing to voltage) because we

can measure extremely weak current fluctuations. The handicap is that we cannot detect fast events or have high temporal resolution. However, the same interesting biological process occurs in a relatively slow time scale, usually less than one event per second [57], [58].

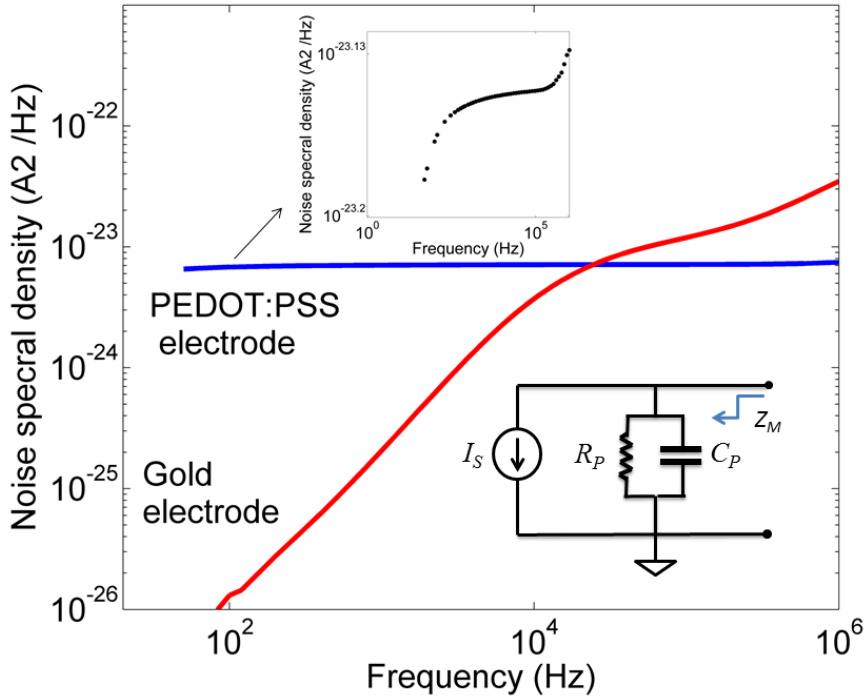

Fig. 4.1 — The noise spectral density of two types of measuring electrodes, gold and printed PEDOT:PSS electrodes on glass. One of the insets shows the equivalent RC network. The other inset shows an expanded view of the PEDOT:PSS noise specral density.

4.3 Results

The performance of our sensing electrodes is illustrated in Fig. 4.2. This figure shows a time trace in which several bursts of noise with amplitudes of 10pA (peak-to-peak) are clearly visible in a noise floor of 4pA (peak-to peak). This time trace was recorded using gold microelectrode arrays and C6 cells. The bursts of noise appear spontaneously.

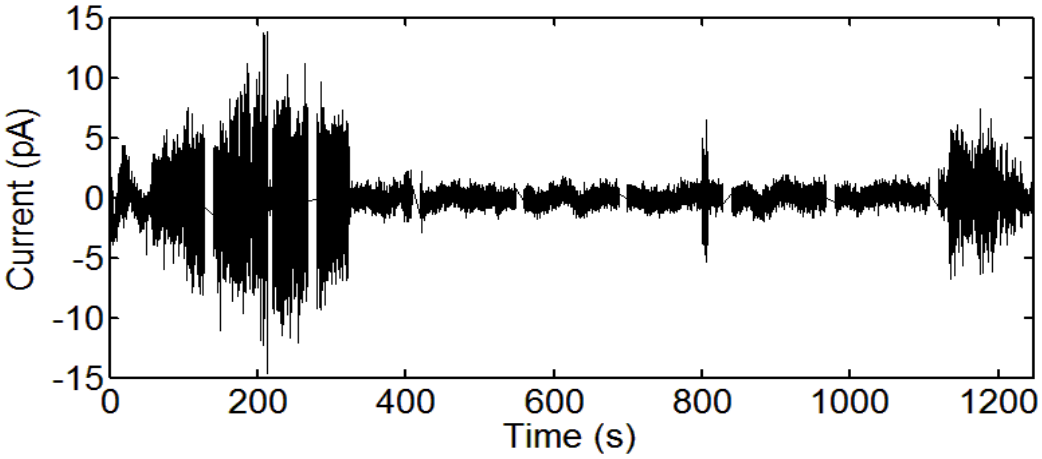

Fig. 4.2 — Time trace of the current recorded using gold microelectrode arrays and C6 cells. Bursts of noise are plainly visible in a noise floor of 4pA (peak-to peak).

To test our sensing method as a drug-screening platform it is convenient to show that the electrical noise can be triggered using chemical stimulus. Fig 4.3 shows the effect on the electrical current triggered by the addition of 2μM of tetrodotoxin (TTX). TTX is a blocker of voltage-sensitive sodium channels. The addition of TTX to the cells resulted in an immediate change in current. However, before they died, a significant increase in the electrical noise was observed. These experiments have been carried out in C6 cells and gold microelectrode arrays as sensing electrodes. The sensing electrodes have been described in Chapter 2.

The addition of KCl to the Neuro-2A cells also resulted in an immediate change in current. KCl was used resulting in a dramatically noise increase which, in turn, caused a depolarization of the membrane of the cell as shown in Fig. 4.4.

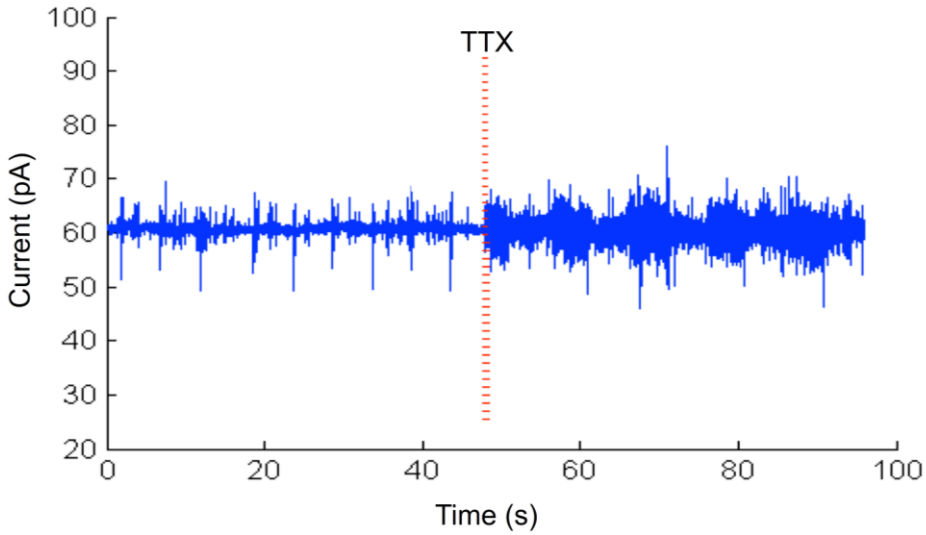

Fig. 4.3 — Time trace of the current measured in C6 cells before and after the exposure to a solution of tetrodotoxin. The sensing electrodes are gold microelectrodes as described in Chapter 2.

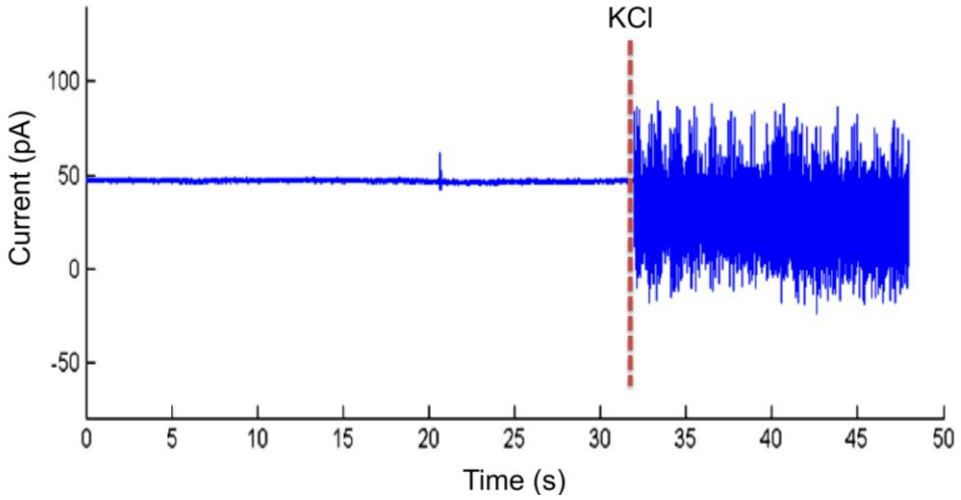

Fig. 4.4 — Chemical induced activity in Neuro-2a cells. Adding a solution 30mM of KCl to the cell culture medium carried out the stimulus. After the addition of a KCl solution the noise increased dramatically.

4.4 Discussion and Conclusion

In conclusion, to measure low frequency and ultra-weak electrical fluctuations generated by the cells, it is important to reduce the electrical noise of the sensing electrodes. This noise is controlled by the resistance of the Helmholtz interfacial layer and varies inversely to the resistance. Therefore, when measurements are carried out in current mode, it is not desirable to have low resistance electrodes. Ideally, the minimum value of the resistance is the one that has a noise level below the electronic instrumentation.

By assuring that the noise of the electrodes is not a limiting factor, ultra-weak electrical fluctuations can be measured. Upon exposure to some chemicals, these electrical fluctuations increase in magnitude and in frequency. As shown and expected, after exposure to TTX, the cell's activity stopped and when the cells were in contact with KCl the noise increased significantly. This may open an interesting opportunity to fabricate non-invasive platforms for drug screening platforms based on electrical noise techniques.

CHAPTER 5

Quasi-Periodic Spikes in Glioma Cells

Measuring the electrical activity of large populations of cells is currently a technical challenge to electrophysiology. For this purpose, a bidirectional transducer based on a metal/Si/SiO_2/interdigitated gold electrode was developed and applied to excite and record long term spike patterns in cultured C6 cells. It is generally assumed that, unlike neurons and non-transformed glia cells, glia cells are not electrically excitable. Yet, it is also known that glioma patients often suffer from epileptic seizures due to the impact of the tumour on brain electrophysiology. With this setup, we determined that glioma cells are capable of firing spikes after electrical perturbation of the cell/dielectric interface with AC coupled voltage pulses, triggering quasi-periodic bursts with inter-spike intervals of approximately 5 seconds (f=0.2Hz). Glia cells display a form of excitability that is based on variations of the Ca^{2+} concentration. An increase in Ca^{2+} in a single cell leads to increases in Ca^{2+} in the surrounding cells, a phenomenon that has been referred to as intercellular calcium waves (ICW). Strikingly, in the absence of any electrical stimuli, glioma cells also engage in spontaneous activity, which evolves from a non-periodic and slow firing rate in a time scale of minutes to a stronger bursting pattern in a time scale of seconds. This spontaneous burst activity is similar to the stimulated one in its amplitude and in its inter-spike intervals in a frequency range of 0.2-0.7Hz. Finally, we were able to correlate the onset of this spontaneous burst activity to a reduction of extracellular pH, which was previously reported to induce ion currents in glioma cells.

5.1 Introduction

This methodology permits simultaneous, non-invasive, long-term recordings of extracellular field potentials generated by an entire cell population. This allows understanding how neuronal ensembles function and how they generate or process spatio-temporal action potential patterns. When non-invasive electrical stimulation is required, electrolyte-oxide-semiconductor field-effect transistors or capacitors are used.

Capacitively coupled voltage ramps have been used to induce membrane current oscillations in cells and can also be used for recording signals. In this approach, cells are placed on top of the open gate of the transistors and stimulated with a micropipette electrode. A two-way communication interface using capacitors for stimulation and transistors for recording was reported [59].

All living cells maintain a membrane potential with a negatively charged cell interior vs. positively charged cell exterior. Fluctuations of the membrane potential play a prominent function, particularly in cells of the nervous system, and are caused by the flux of primarily Na^+, K^+ and Ca^{2+} ions along the gradient, controlled by the function of various ion channel protein families. In neurons, depolarisations of membrane potential can reach a reversal of electric polarity of the cell membrane, known as action potential, which was already explained in chapter 2. Yet, glial cells have long been demonstrated to act as express voltage gated channels and to be electrically active individually [60]. It is also important to bear in mind that, even if glia cells cannot produce an action potential, their excitability and membrane depolarisations are highly functional [61], e.g. by controlling glia-mediated neurotransmitter uptake and release [62].

Several types of sensing electrodes and electronic devices have been developed to study cells *in vitro*. Microelectrode Arrays (MEAs) technology is now considered a standard method for extracellular recording and stimulation of neural activity, as demonstrated by many electro-physiology studies in the domain of neuroscience. This methodology permits simultaneous, cell-non-invasive, long-term recordings of extracellular field potentials generated by an entire cell population. This enables to understand how neuronal ensembles function and how they generate or process spatio-temporal action potential patterns.

Brain tumour-derived glioma/glioblastoma cells still retain many characteristics of their untransformed counterparts, including the expression of neurotransmitter receptors and voltage-gated ion channels [63]. Additionally, Glioma patients often a suffer from epileptic seizures, which is thought to be caused due to the release of neurotransmitters by the tumour cells [64]. Given that such processes in healthy glia are controlled by membrane depolarisation events [62], it is important to understand to what extent brain tumour bulk cells are involved in their own electrophysiological activities. The technical status of the electrophysiology research is focused on the observation of electrical activity on a single cell level, i.e. patch-clamp method. This approach, however, does not allow assessment of membrane fluctuations of an entire large population of a defined cell type.

Here, we present a bidirectional transducer that can electrically stimulate and measure external membrane current fluctuation of a uniform cell population, using a well-defined rat glioma cell line C6 as a model system. The transducer uses a thin dielectric layer to excite the entire cell population and an interdigitated electrode to record the signals in a full planar design. Two strategies of bidirectional MEAs electrodes are commonly in use; the simpler one employs electrodes that can be switched between recording and stimulation. The limitation of this approach is that a minimum settling time must be allowed when the electrodes switch from stimulation to recording mode. In the other approach, a second subset of electrodes is connected nearby or outside the recording electrode array allowing the delivery of voltage or pulse currents to cells as demonstrated by [65], [66]. Our approach to electrically stimulate cells is similar to the one presented by [67] using an electrolyte-oxide-semiconductor capacitor. Our bidirectional transducer ablates the necessity of external patch clamp micropipettes to record the induced cells signals. We are able to stimulate and record a large population of cells and thereby elicit the synchronization of intercellular signals and other cooperative phenomena.

Glia cells display a form of excitability that is based on variations of the Ca^{2+} concentration. An increase in Ca^{2+} in a single cell leads to increases in Ca^{2+} in the surrounding cells, a phenomenon that has been referred to as intercellular calcium waves (ICW). Calcium waves have been demonstrated using a variety of stimuli including mechanical and chemical [68]. Although it has been shown that calcium signals can be electrically elicited in neurons [69], the same has never been

demonstrated in glia cells. ICWs can be initiated by local stimulation of a single cell or by the global stimulation of a population of cells. Local initiation has been achieved by mechanical stimulation of a cell with a micropipette; which we argued results in membrane stress that triggers the production of inositol 1,4,5-trisphosphate [70]. ICWs may also be triggered by extracellular factors, i.e. pH changes as observed in brain stem slices, which display ICWs in response to a lowering of the extracellular pH. ICWs can also occur spontaneously, *in vitro*.

The speed and size of ICWs depend on the nature and strength of the initiating stimulus as well as on the mechanism of propagation. ICW's often propagate for periods of up to tens of seconds with speeds of 10–20μm/s. Ca^{2+} waves can frequently pass between disconnected cells as long as the gap between them does not exceed ~120μm [71]. Several studies using digital fluorescence video microscopy have reported random spikes of spontaneous calcium oscillations as well as synchronized operation with frequencies below 1Hz.

5.2 Results

The transducer is based on a capacitor-like device. The top surface where cells adhere is comprised of interdigitated Au electrodes deposited on an insulating SiO_2 surface. The cells adhere equally well to the electrodes and the SiO_2 interface. For the measurements, each surface is used separately. The insulating silicon surface is used for capacitive stimulation. The interdigitated Au electrodes are used to sense electrical changes at the cells/Au interfaces. When voltage pulses were applied to the silicon substrate the symmetric top Au electrodes were kept grounded to avoid Faradic currents and redox reactions. After external electrical stimulation, the gate terminal is grounded and the signals between the Au microelectrodes are recorded. The transducer is connected to a homemade chip holder, which incorporates a commercially available Petri dish for cell culture. The system assures the presence of enough cell culture medium to keep the cells viable over more than 10 hours without medium change.

Cell adhesion to the microelectrode arrays was monitored using small-signal impedance. Fig. 5.1 shows the frequency dependence of the admittance. The data is represented for both the equivalent parallel capacitance, C, and loss, G/ω where G is the conductivity and ω the angular frequency, $2\pi f$. Two sets of curves are shown; one

measured at the early stages of the cell adhesion and a second set measured 145 minutes later when the adherent cells have already coated the microelectrodes. For both sets of curves the frequency dependence has a dispersion or relaxation centred at a particular frequency (*fr).* This dispersion in the admittance appears because the system behaves as a two-layer system, comprised of a high capacitance and high resistance interfacial region (Helmholtz-Gouy or Stern double-layer) in series with a low capacitance and lower resistance electrolyte solution [72], [73].

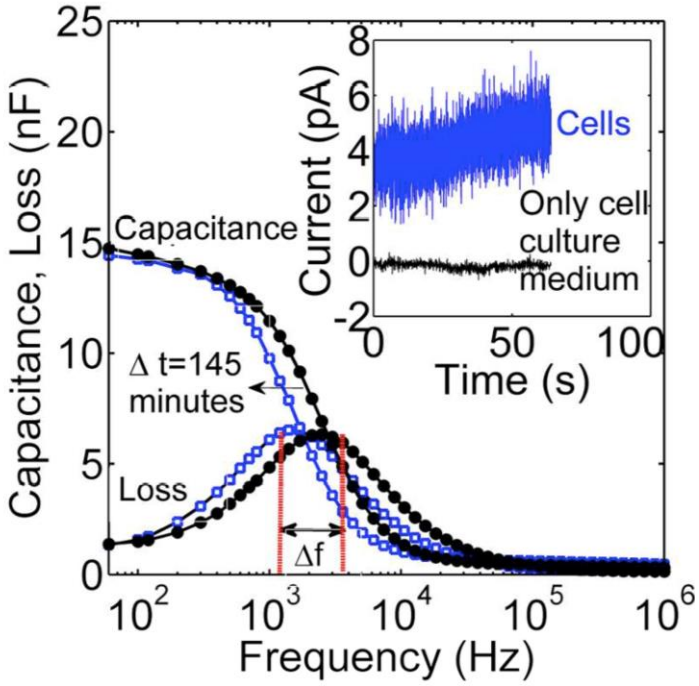

Fig. 5.1 — Frequency dependence of the capacitance (C) and loss (1/Rω). As the cells adhere to the sensing electrodes, the Maxwell-Wagner relaxation moves to lower frequencies. The inset shows a time trace of the noise current fluctuations when the C6 cells are resting and adherent to the microelectrodes.

The Maxwell-Wagner relaxation frequency, f_r, is determined by the resistance of the cell culture medium. The resistance depends essentially on the geometrical parameters of the sensing electrodes such as the active area and the distance between the electrodes. As cells adhere to the electrodes, the relaxation frequency shifts to lower frequencies. As shown in Fig. 5.1, the shift, Δf_r, is about 2kHz. This shift occurs because the cell membrane is insulating and impedes the AC conductance [74].

First, we addressed the question whether C6 cell cultures can be stimulated electrically. For this, we applied voltage pulses across the gate dielectric. Fig. 5.2a shows spikes of cell activity recorded after the application of a train of pulses (5V, 200s for 2 minutes).

Initially, relatively weak and non-periodic bursts embedded in thermal noise were observed. After a few minutes the spikes rose in amplitude and became more frequent. A zoom-in reveals that the signals can be quasi-periodic over time, with spans as long as 60s. Fig. 5.2b shows an example of a quasi-periodic signal with an average inter-spike interval of 5s. The firing rate is approximately 0.2Hz and the average amplitude is 40pA peak-to-peak. The spikes are bipolar with up- and downward oscillations centred in a direct current (DC)-offset. This contrasts with the unipolar signals discussed in Fig. 5.3. The reason for this disparity lies in the use of different instrumentation. The unipolar signals in Fig. 5.3 where recorded using a non-floating picoammenter, while the bipolar signals shown in Fig. 5.2 were recorded using a floating differential amplifier.

Fig. 5.2c shows several time traces, each with an individual length of 60s. These traces were recorded sequentially in time from the bottom trace (A) to the top trace (G). They resume a typical behaviour of the spike amplitude and periodicity. This activity is triggered by a train of voltage pulses across the dielectric layer. Trace (A) was recorded just prior to stimulation and shows that cells are resting. Trace (B) was recorded after capacitive stimulation. Small and non-periodic bursts of activity are observed. Later on, these bursts increase in amplitude as shown in trace (C). The bursts evolve to quasi-periodic signals (0.2Hz) as shown in trace (D) and (E).

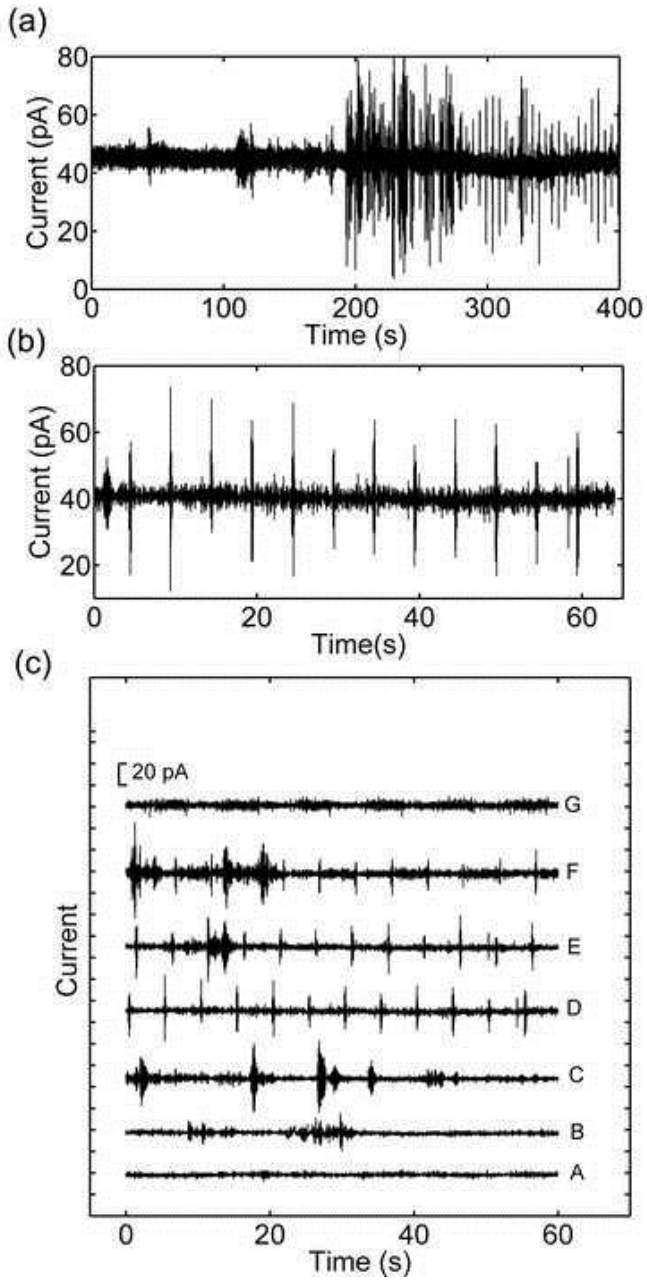

Fig. 5.2 — Stimulated cell activity. (a) Time dependence of the current recorded after the application of a train of voltage pulses (5 V, 200μs for 2 minutes), (b) a quasi-periodic signal with a frequency approximately of 0.2Hz. Electrical measurements were carried out using the floating differential amplifier. (c) Consecutive traces with individual lengths of 60s recorded from the bottom to the top. Trace (A) shows a pure thermal noise. Trace (B) is recorder after capacitive stimulation; small and non- periodic burst of activity are observed. Later in trace (C) the burst increase in amplitude and evolve to a perfect periodic activity as shown in traces (D) and (E). The signals can be stopped upon the addition of ethylenediamine tetraacetic acid (EDTA) as shown in trace (G).

Electrical activity of glial cells often involves the flux of extracellular Ca^{2+} ions through specific channels [60]. On a single-cell level, Ca^{2+} ion flux was shown to be relevant for membrane currents in C6 cells during cell swelling [75]. We depleted extracellular Ca^{2+}

by supplementing cell culture medium with of a Ca^{2+} chelate agent EDTA (0.1mM). Approximately 9 minutes after the addition of EDTA, the bursting activity was inhibited and the electrical signal returned to the background thermal noise as shown in trace (G). This confirms the need of Ca^{2+} ion flux for the electric activity in C6 cells.
Remarkably, spontaneous electric activity of C6 cells was also detected approximately 5 hours after cell deposition, in absence of any external electrical stimulation. The electrical response analysis over time is shown in Fig. 5.3a and reveals a complex behaviour. The pattern of the signals varies substantially over time. The activity can be characterized into 4 consecutive time regions with clear distinct spike patterns. The onset of the activity (region I in Fig. 5.3a) is characterized by weak (5-10pA) sporadic spikes separated by time intervals that can be as long as 5 minutes. This slow and weak activity gives rise to a second pattern characterized by an increase of the firing rate and magnitude of the spikes (region II).

The amplitude of the spikes rises from 10pA to 80pA (similarly to stimulated cells shown before) and the time intervals can be as short as a few seconds. This rise in activity lasts for more than 1000s. Then the activity stops for a few minutes, which is considered a silent region, and it is followed by an apparent chaotic behaviour (region III). In this region, the time intervals between spikes can be as short as 2-4 seconds. Although the overall pattern looks random, a detailed view reveals short time regions where the spike pattern becomes quasi-periodic with frequencies below 0.5Hz.

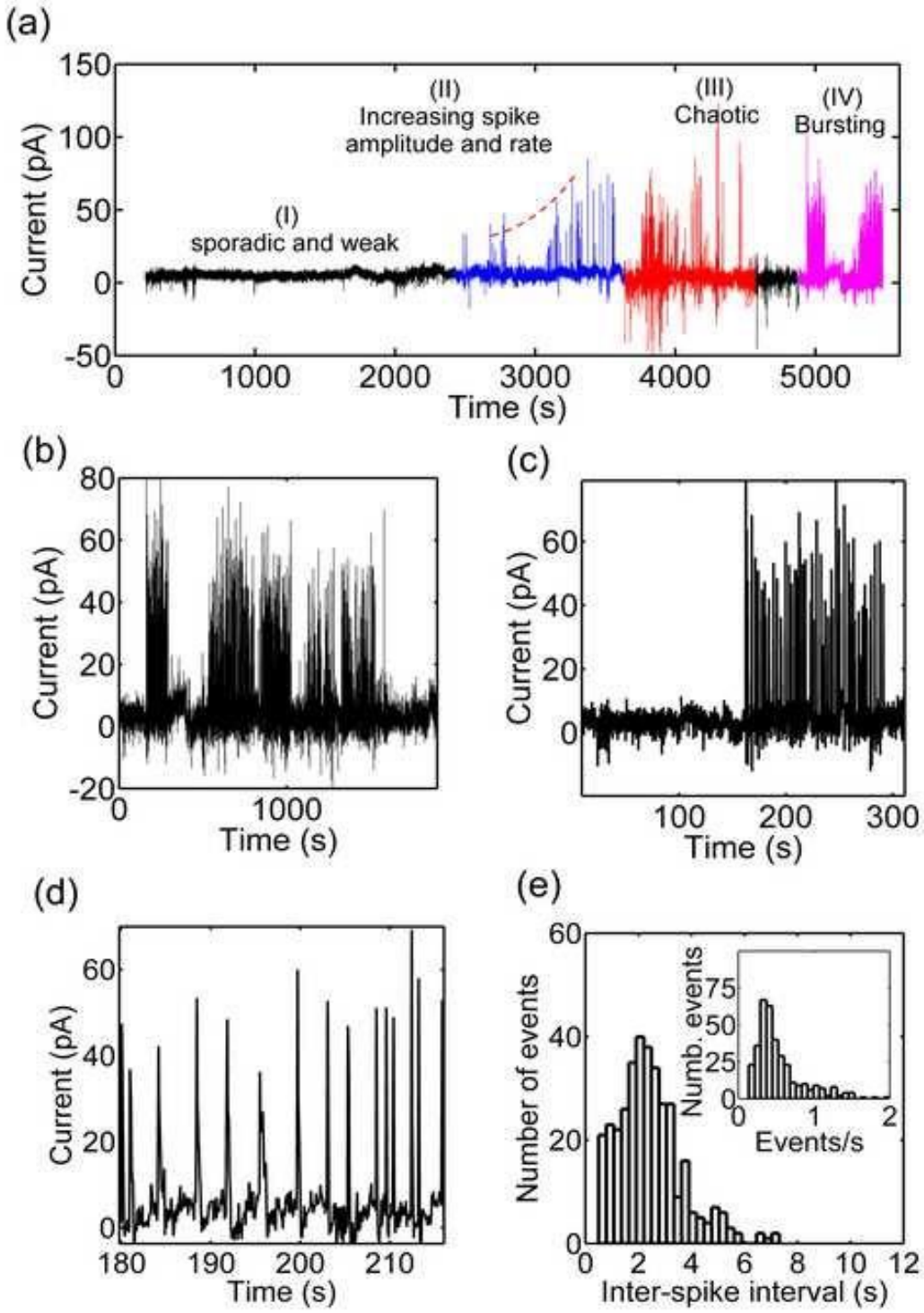

Fig. 5.3 — (a) Evolution of the magnitude and frequency of the spikes with time for a spontaneous activity; four distinct periods of activities can be detected. (b) Bursting activity, (c) view of an individual burst and (d) detailed view of quasi-periodic spikes inside the burst. The inter-spike interval is 3.3 s (0.3Hz). (e) Histogram of the inter-spike intervals recorded for the entire burst activity shown in (a). The inter-spike intervals were distributed into time slots with a resolution of 0.33s. The inset shows the histogram of the corresponding frequencies.

Approximately one hour after the onset of cell activity the spike pattern evolves into a bursting behaviour, region IV. The spikes appear now in clusters separated by silent regions. Both the bursts, as well as the silent regions, can be as long as 100-200 seconds. As shown in Fig. 5.3b-d, within the individual bursts, the spikes reveal a quasi-periodic behaviour. Fig. 5.3b shows a time trace of a typical bursting activity. A zoom-in of an individual burst is shown in Fig. 5.3c. An expanded view is presented in Fig. 5.3d. The spikes are approximately equidistant, with an inter-spike interval of approximately 0.4s. However, there are also spikes that appear either randomly or separated by shorter times.

In order to identify firing patterns, we performed the following analysis. For the entire time trace of Fig. 5.3b we measured the time between two consecutive spikes. These inter-spike intervals were then counted and distributed into time slots with a resolution of 0.33s. Time intervals shorter than 0.33s and longer than 8s were not considered because they were rare. Fig. 5.3e shows the histogram of the number of spikes counted in each inter-spike interval. Spikes separated by time intervals between 1.98s and 3.3s have the highest number of counts. A second small peak appears for time lengths of 3.96s (f=0.5Hz). The inset of Fig. 5.3e shows the inter-spike intervals converted into the corresponding frequencies. The distribution of events is centred at the frequency of 0.3-0.4Hz. In order to test whether the recordings of electrical activity in C6 cultures can be traced back to apoptosis and associated with membrane-depolarizing events, we performed cell growth and viability assays. As Fig. 5.4a shows, cell numbers rapidly increased almost 10 fold 24h after deposition, while the average vitality of the cultures remained at all points around ~80% (±12%). Moreover, we detected a rapid cell culture medium acidification already several hours after cell deposition. In fact, the reduction in culture medium pH value could be already observed by the colour change of the commercially supplemented pH-indicator phenol red towards a yellow colour shade.

To investigate this observation, we performed kinetics studies of the pH development in the wells containing C6 cells, as opposed to cell-free medium. As Fig. 5.4b shows, cell culture medium acidification began soon after cell deposition, when the cell number has roughly tripled. Remarkably, a major drop in pH value could be correlated to the onset of spontaneous electric burst activity in the glioma cells.

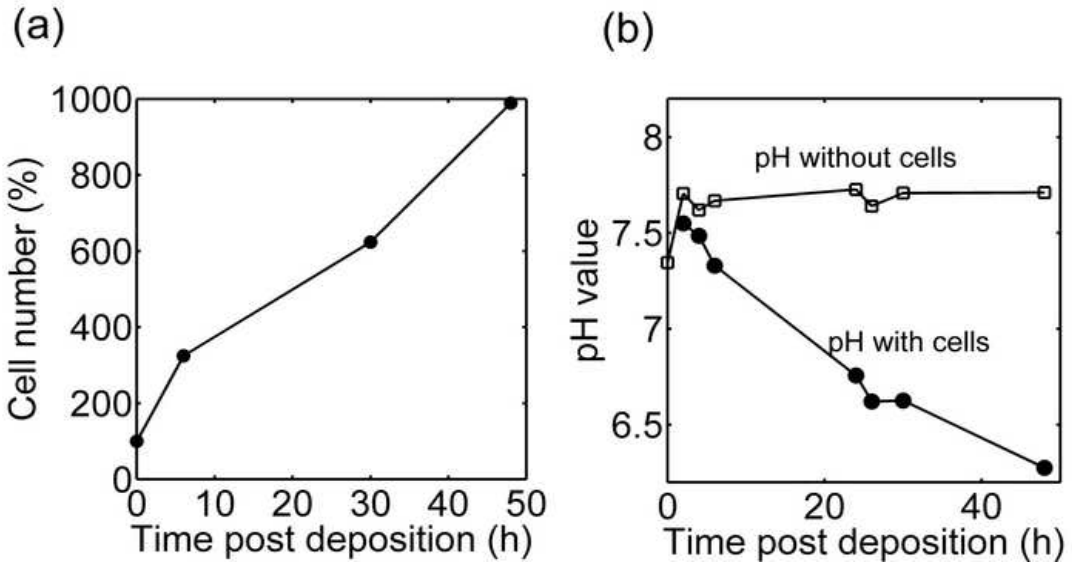

Fig. 5.4 — Kinetics of cell growth (a) and cell metabolism-related pH changes in culture medium (b). $2.3x10^5$ cells were seeded initially in a volume of 200µl. Average cell vitality was 79% (±12%). Results provided by a partner (Paulo Rocha at Max Planck Institute for Polymer Research).

5.3 Discussion

Our technical setup allows the recording of the electrical activity of an entire cell population using a bidirectional transducer. With its help, we could determine here that C6 cells are electrically excitable by AC coupled voltage pulses. We provide evidence into ion flux nature of these currents by proving the requirement of extracellular Ca^{2+} ions for the burst activity. After stimulation, episodes of synchronous firing (0.2 Hz) are frequently observed. This suggests that the cells become synchronized when the cell/substrate interface is electrically charged. Moreover, C6 cells also engage in spontaneously electrical activity, which also generates bursts of current spikes of high amplitude. Occasionally these spontaneous signals also show brief quasi-periodic behaviour, the repetition rate being between 0.2 to 0.4 spikes per second. These electric activities are strikingly similar to those induced by AC coupled voltage pulses, which indicates a cell culture-intrinsic coordination stimulus. Fundamentally, we demonstrate that this phenomenon is not associated with cell death; in fact, cells are highly viable and proliferative when the spontaneous electric activity is observed.

Our findings that a population of C6 cells is not only responsive to electric stimulation,

but can also engage in spontaneous electric activity, independent of any neuronal or experimental stimuli, may be highly relevant for the understanding of the tumours impact on brain electrophysiology. In particular, the high incidence of seizures in glioma patients [64] and observations that glioma directly interfere with the electrophysiology of the surrounding brain tissue [76], make our experimental data particularly intriguing. Since glioma cells are, apparently, not electrically inert after all, and can spontaneously engage in a remarkable burst activity, this is likely to directly perturb the functionality of the healthy neuronal network in the vicinity of the tumour bulk. Alternatively, glioma cells may disrupt brain functionality indirectly by producing seizure-inducing neurotransmitters, of which primarily glutamate is a very strong candidate [64], [77]. Glutamate release is commonly controlled by astroglia, where Ca^{2+} and Na^{+} ion flux results in the release of the vesicular glutamate into the extracellular/synaptic space (Montana et al. 2004). C6 cells were in fact shown to release glutamate upon extracellular ion stimulation [77]. Since we offer here the phenotypical evidence for ion-mediated electric currents in glioma cell cultures, it is highly likely that such tremendous electric activity may result in vesicular neurotransmitter release from glioma cells. Therefore, we propose further investigations whether epileptic seizures may indeed be caused by the intrinsic electric activity of glioma and their subsequent neurotransmitter release.

Our data indicates a correlation between increased cell numbers and a drop in extracellular pH of the buffered culture medium. Practical life science laboratory experience postulates that such culture medium acidification is caused by the increased metabolism of rapidly dividing cell cultures, in particular transformed and contact-uninhibited cells (which C6 cells clearly are). Thus, we believe that the onset of the spontaneous electric activity in glioma cultures is likely to be primarily caused by this extracellular acidification. Indeed, C6 do respond to pH changes by ion currents across the cell membrane [56], [78]. Moreover, glioma cells, including C6, were shown to express functional acid-sensing ion channels (ASICs), which respond to elevated extracellular proton concentration (e.g., acidified culture medium) by allowing inward Na^{+} ion currents [79]–[82]. These studies have proven that C6 cells respond to elevated extracellular pH by ASIC-mediated Na^{+} ion flux and membrane currents on a single-cell level. Correspondingly, our data demonstrates a concerted burst activity in entire glioma cultures, neatly associated with reduced extracellular pH. This is intriguing as

tumours with their disorganized vasculature and fast growth display a strongly acidic extracellular environment to buffer their hypoxia-induced production of lactic acid [83], such pH gradient was also observed in C6 glioma *in vivo* [84]. Therefore, it is reasonable to assume that our findings reflect a potential mechanism for epileptic events in glioma patients.

5.4 Conclusions

In summary, we have shown that quasi-periodic oscillations, both spontaneous and stimulated, can be excited and recorded in glioma cultures using a planar device and electrical methods. The bidirectional transducer represents an advance with respect to conventional MEAs because it allows both the excitation and the monitoring of electric activity of an entire defined population of cells. Moreover, our discovery of acidity-associated spontaneous electric burst activity in glioma cells bears high relevance for the understanding of the detrimental impact of brain tumours on the patient's brain function, such as commonly observed epileptic seizures.

CHAPTER 6

Conclusions

6.1 Conclusions

This thesis focused on the matter of using electrical techniques to monitor cells *in vitro*. The prime goal was to optimize materials and the devices in order to fabricate electronic devices capable to perform extracellular recordings of ultra-weak signals.

For that purpose, we tested and characterized a number of sensing electrodes based on a variety of materials, including metals and conducting polymers.

Regarding test cells, two types of neuronal cell lines were utilised, specifically neurons and glioma cells. The following important results were obtained:

1- By using small signal impedance techniques we gained insight into how to optimize the individual impedance parameters to achieve high sensitivity. In this case, the major finding was that, after performing measurements in current mode, we realized that the capacitance must be maximized; however, the resistance has to be relatively high to reduce the electrode's noise. This optimization of the electrode impedance can be achieved by using printed polymer electrodes. By controlling the printing setting parameters, it was also possible to control the surface's roughness and the impedance.

2- It was also shown that ink-jet printed PEDOT:PSS electrodes are an easy and low-cost method to create sensing electrodes. To record extracellular signals, polymer-based electrodes perform better than gold electrodes.

3- Preliminary data had shown strong evidences that with a proper selection of electrodes and the use of high gain amplifiers it is possible to detect ultra-weak electrical fluctuations of cell cultures. The testes carried out in glioma cells cultures and in Neuro-2a demonstrate that the frequency and the amplitude of the bioelectrical noise increase when the cells are exposed to toxic substances. Given this results it can be asserted that noise can be used as a drug-screening platform.

4- The study of glioma cells cultures has revealed that these cells can exhibit electrical activity. This activity is characterized by a burst of quasi-periodic signals often intercalated by silent regions. Traces of activity have been measured for periods as long as hours. These findings are particular interesting because, to the best of our knowledge, electrical activity in these cells has not to be reported before. Thus, it can be concluded at these electrical signals are related to travelling calcium waves.

6.2 Suggestions for further work

6.2.1 Observation of low frequency and ultra weak extracellular signals

The observation of extracellular calcium waves using electrical methods opens a fascinating unexplored area. The scientific community has relatively neglected these low frequency and ultra signal communication pathways between cells. The emphasis is on strong and relatively high frequency signals generated by neurons (action potentials). Furthermore, the calcium wave signaling has only been reported using fluorescence imaging. This method requires complicated protocols (use of optical dyes). Usually the window of observation is limited to a few hours at best. Electrical techniques, however, do not require a cell labeling, are totally non-invasive and can follow the cells in real time for longer, extended periods of time (weeks). Based on our research, we believe that we can offer the scientific community a new tool to address a whole range of low frequency events that the cells used to communicate and to coordinate their activities. There are strong evidences that the low frequency signal is involved in a number of diseases such as Alzheimer disease, Parkinson disease or Brain cancer.

6.2.2 Drug screening platform

It is shown in chapter 4 that the noise can be used to monitor chemical induced changes. It would be interesting to make a record of the behaviour of certain types of cells in a wider range of drugs. This procedure would allow us to start creating a library of signals for cellular response to drugs.

6.2.3 Prosthetic and electroceutical devices.

Understanding how neurons produce our thoughts, perceptions, and actions is one of the greatest challenges of science. When this activity is disrupted, it gives rises to neurological and psychiatric disorders. Brain-related illnesses affect more than two billion people worldwide. Advances in treatments for brain disorders have to date relied largely on a pharmaceutical approach; however, the development of drugs, which do not have intolerable side effects, is becoming extremely complex and difficult. It is now believed that and electronic engineering-driven approach is needed to develop solutions based on electrical signals. This is supported by a number of progresses in electronic

transducers working as prosthetic and electroceutical devices. These are devices that aim to establish an electrical and chemical bidirectional communication interface with cells and tissues. Once the signals are decoded, devices can also generate the correct signal patterns to modulate the neural impulses controlling the body, repair lost connections and restore function.

6.2.4 Implantable devices

The results in this thesis can be easily applied to devices fabricated in a flexible, conformable and biocompatible scaffold as in the iONE-FP7 Project. It will be interesting to explore the performance of electrodes fabricated using polymers in bacterial cellulose substrates for *in vivo* experiments.

CHAPTER 7

References

[1] E. Giusto, M. Donegà, C. Cossetti, and S. Pluchino, “Neuro-immune interactions of neural stem cell transplants: From animal disease models to human trials,” *Exp. Neurol.*, vol. 260, pp. 19–32, 2013.

[2] M. Casadio, a Pressman, S. Acosta, Z. Danzinger, a Fishbach, F. a Mussa-Ivaldi, K. Muir, H. Tseng, and D. Chen, “Body machine interface: remapping motor skills after spinal cord injury.,” *IEEE Int. Conf. Rehabil. Robot.*, vol. 2011, p. 5975384, 2011.

[3] N. A. Silva, N. Sousa, R. L. Reis, and A. J. Salgado, “From basics to clinical: A comprehensive review on spinal cord injury,” *Progress in Neurobiology*, vol. 114. pp. 25–57, Mar-2014.

[4] F. H. Gage, “Mammalian Neural Stem Cells,” *Science*, vol. 287, no. 5457. pp. 1433–1438, 2000.

[5] P. Lu, L. L. Jones, E. Y. Snyder, and M. H. Tuszynski, “Neural stem cells constitutively secrete neurotrophic factors and promote extensive host axonal growth after spinal cord injury,” *Exp. Neurol.*, vol. 181, no. 2, pp. 115–129, 2003.

[6] M. G. Fehlings and R. Vawda, “Cellular Treatments for Spinal Cord Injury: The Time is Right for Clinical Trials,” *Neurotherapeutics*, vol. 8, no. 4, pp. 704–720, 2011.

[7] T. R. Brazelton, F. M. Rossi, G. I. Keshet, and H. M. Blau, “From marrow to brain: expression of neuronal phenotypes in adult mice.,” *Science*, vol. 290, no. 5497, pp. 1775–1779, 2000.

[8] E. Mezey, K. J. Chandross, G. Harta, R. a Maki, and S. R. McKercher, “Turning blood into brain: cells bearing neuronal antigens generated in vivo from bone marrow.,” *Science*, vol. 290, no. 5497, pp. 1779–1782, 2000.

[9] D. Woodbury, E. J. Schwarz, D. J. Prockop, and I. B. Black, “Adult rat and human bone marrow stromal cells differentiate into neurons.,” *J. Neurosci. Res.*, vol. 61, no. 4, pp. 364–370, 2000.

[10] W. Tetzlaff, E. B. Okon, S. Karimi-Abdolrezaee, C. E. Hill, J. S. Sparling, J. R. Plemel, W. T. Plunet, E. C. Tsai, D. Baptiste, L. J. Smithson, M. D. Kawaja, M. G. Fehlings, and B. K. Kwon, “A systematic review of cellular transplantation therapies for spinal cord injury.,” *J. Neurotrauma*, vol. 28, no. 8, pp. 1611–1682, 2011.

[11] L. Urdzíková, P. Jendelová, K. Glogarová, M. Burian, M. Hájek, and E. Syková, “Transplantation of bone marrow stem cells as well as mobilization by granulocyte-colony stimulating factor promotes recovery after spinal cord injury in rats.,” *J. Neurotrauma*, vol. 23, no. 9, pp. 1379–1391, 2006.

[12] M. Ohta, Y. Suzuki, T. Noda, Y. Ejiri, M. Dezawa, K. Kataoka, H. Chou, N. Ishikawa, N. Matsumoto, Y. Iwashita, E. Mizuta, S. Kuno, and C. Ide, "Bone marrow stromal cells infused into the cerebrospinal fluid promote functional recovery of the injured rat spinal cord with reduced cavity formation," *Exp. Neurol.*, vol. 187, no. 2, pp. 266–278, 2004.

[13] F. Féron, C. Perry, J. Cochrane, P. Licina, A. Nowitzke, S. Urquhart, T. Geraghty, and A. Mackay-Sim, "Autologous olfactory ensheathing cell transplantation in human spinal cord injury.," *Brain*, vol. 128, no. Pt 12, pp. 2951–60, 2005.

[14] R. Doucette, "PNS-CNS transitional zone of the first cranial nerve.," *J. Comp. Neurol.*, vol. 312, no. 3, pp. 451–66, 1991.

[15] C. Lima, J. Pratas-Vital, P. Escada, A. Hasse-Ferreira, C. Capucho, and J. D. Peduzzi, "Olfactory mucosa autografts in human spinal cord injury: a pilot clinical study.," *J. Spinal Cord Med.*, vol. 29, no. 3, pp. 191–203; discussion 204–6, 2006.

[16] M. B. Bunge, "Novel combination strategies to repair the injured mammalian spinal cord.," *J. Spinal Cord Med.*, vol. 31, no. 3, pp. 262–269, 2008.

[17] M. Oudega and X.-M. Xu, "Schwann cell transplantation for repair of the adult spinal cord.," *J. Neurotrauma*, vol. 23, no. 3–4, pp. 453–467, 2006.

[18] I. Shaked, Z. Porat, R. Gersner, J. Kipnis, and M. Schwartz, "Early activation of microglia as antigen-presenting cells correlates with T cell-mediated protection and repair of the injured central nervous system," *J. Neuroimmunol.*, vol. 146, no. 1–2, pp. 84–93, 2004.

[19] O. Rapalino, O. Lazarov-Spiegler, E. Agranov, G. J. Velan, E. Yoles, M. Fraidakis, A. Soloman, R. Gepstein, A. Katz, M. Belkin, M. Hadani, M. Schwartz, and A. Solomon, "Implantation of stimulated homologous macrophages results in partial recovery of paraplegic rats," *Nat. Med.*, vol. 4, no. 7, pp. 814–821, 1998.

[20] O. Butovsky, A. E. Talpalar, K. Ben-Yaakov, and M. Schwartz, "Activation of microglia by aggregated β-amyloid or lipopolysaccharide impairs MHC-II expression and renders them cytotoxic whereas IFN-γ and IL-4 render them protective," *Mol. Cell. Neurosci.*, vol. 29, no. 3, pp. 381–393, 2005.

[21] B. J. Conley, J. C. Young, A. O. Trounson, and R. Mollard, "Derivation, propagation and differentiation of human embryonic stem cells.," *Int. J. Biochem. Cell Biol.*, vol. 36, no. 4, pp. 555–67, 2004.

[22] J. W. McDonald, X. Z. Liu, Y. Qu, S. Liu, S. K. Mickey, D. Turetsky, D. I. Gottlieb, and D. W. Choi, "Transplanted embryonic stem cells survive,

differentiate and promote recovery in injured rat spinal cord.," *Nat. Med.*, vol. 5, no. 12, pp. 1410–1412, 1999.

[23] S. Liu, Y. Qu, T. J. Stewart, M. J. Howard, S. Chakrabortty, T. F. Holekamp, and J. W. McDonald, "Embryonic stem cells differentiate into oligodendrocytes and myelinate in culture and after spinal cord transplantation.," *Proc. Natl. Acad. Sci. U. S. A.*, vol. 97, no. 11, pp. 6126–6131, 2000.

[24] J. W. McDonald and C. Sadowsky, "Spinal-cord injury," in *Lancet*, 2002, vol. 359, no. 9304, pp. 417–425.

[25] B. H. Dobkin and L. A. Havton, "Basic advances and new avenues in therapy of spinal cord injury.," *Annu. Rev. Med.*, vol. 55, no. 1, pp. 255–282, Feb. 2004.

[26] S. Woerly, D. Van Doan, F. Evans-Martin, C. G. Paramore, and J. D. Peduzzi, "Spinal cord reconstruction using NeuroGel™ implants and functional recovery after chronic injury," *J. Neurosci. Res.*, vol. 66, no. 6, pp. 1187–1197, 2001.

[27] E. C. Tsai, P. D. Dalton, M. S. Shoichet, and C. H. Tator, "Matrix inclusion within synthetic hydrogel guidance channels improves specific supraspinal and local axonal regeneration after complete spinal cord transection," *Biomaterials*, vol. 27, no. 3, pp. 519–533, 2006.

[28] L. F. Reynolds, M. C. Bren, B. C. Wilson, G. D. Gibson, M. S. Shoichet, and R. J. L. Murphy, "Transplantation of porous tubes following spinal cord transection improves hindlimb function in the rat.," *Spinal cord Off. J. Int. Med. Soc. Paraplegia*, vol. 46, no. 1, pp. 58–64, 2008.

[29] H. Nomura, Y. Katayama, M. S. Shoichet, and C. H. Tator, "Complete spinal cord transection treated by implantation of a reinforced synthetic hydrogel channel results in syringomyelia and caudal migration of the rostral stump," *Neurosurgery*, vol. 59, no. 1, pp. 183–192, 2006.

[30] J. Luo, R. Borgens, and R. Shi, "Polyethylene glycol immediately repairs neuronal membranes and inhibits free radical production after acute spinal cord injury," *J. Neurochem.*, vol. 83, no. 2, pp. 471–480, 2002.

[31] R. Shi and R. B. Borgens, "Acute repair of crushed guinea pig spinal cord by polyethylene glycol.," *J. Neurophysiol.*, vol. 81, no. 5, pp. 2406–2414, 1999.

[32] J. Piantino, J. A. Burdick, D. Goldberg, R. Langer, and L. I. Benowitz, "An injectable, biodegradable hydrogel for trophic factor delivery enhances axonal rewiring and improves performance after spinal cord injury," *Exp. Neurol.*, vol. 201, no. 2, pp. 359–367, 2006.

[33] Y. D. Teng, E. B. Lavik, X. Qu, K. I. Park, J. Ourednik, D. Zurakowski, R. Langer, and E. Y. Snyder, "Functional recovery following traumatic spinal cord

injury mediated by a unique polymer scaffold seeded with neural stem cells.," *Proc. Natl. Acad. Sci. U. S. A.*, vol. 99, no. 5, pp. 3024–3029, 2002.

[34] V. M. Tysseling-Mattiace, V. Sahni, K. L. Niece, D. Birch, C. Czeisler, M. G. Fehlings, S. I. Stupp, and J. A. Kessler, "Self-assembling nanofibers inhibit glial scar formation and promote axon elongation after spinal cord injury.," *J. Neurosci.*, vol. 28, no. 14, pp. 3814–3823, 2008.

[35] A. H. Petter-Puchner, W. Froetscher, R. Krametter-Froetscher, D. Lorinson, H. Redl, and M. van Griensven, "The long-term neurocompatibility of human fibrin sealant and equine collagen as biomatrices in experimental spinal cord injury," *Exp. Toxicol. Pathol.*, vol. 58, no. 4, pp. 237–245, 2007.

[36] D. A. Houweling, A. J. Lankhorst, W. H. Gispen, P. R. Bär, and E. A. Joosten, "Collagen containing neurotrophin-3 (NT-3) attracts regrowing injured corticospinal axons in the adult rat spinal cord and promotes partial functional recovery.," *Exp. Neurol.*, vol. 153, no. 1, pp. 49–59, 1998.

[37] X. Li, Z. Yang, A. Zhang, T. Wang, and W. Chen, "Repair of thoracic spinal cord injury by chitosan tube implantation in adult rats," *Biomaterials*, vol. 30, no. 6, pp. 1121–1132, 2009.

[38] H. K. Kleinman and G. R. Martin, "Matrigel: Basement membrane matrix with biological activity," *Semin. Cancer Biol.*, vol. 15, no. 5 SPEC. ISS., pp. 378–386, 2005.

[39] S.-H. Lee, Y.-N. Chung, Y.-H. Kim, Y.-J. Kim, J.-P. Park, D.-K. Kwon, O.-S. Kwon, J.-H. Heo, Y.-H. Kim, S. Ryu, H.-J. Kang, S. H. Paek, K.-C. Wang, S. U. Kim, and B.-W. Yoon, "Effects of human neural stem cell transplantation in canine spinal cord hemisection.," *Neurol. Res.*, vol. 31, no. 9, pp. 996–1002, 2009.

[40] A. Samadikuchaksaraei, "An overview of tissue engineering approaches for management of spinal cord injuries.," *J. Neuroeng. Rehabil.*, vol. 4, p. 15, 2007.

[41] S. J. Taylor, J. W. McDonald, and S. E. Sakiyama-Elbert, "Controlled release of neurotrophin-3 from fibrin gels for spinal cord injury," *J. Control. Release*, vol. 98, no. 2, pp. 281–294, 2004.

[42] H. Kim, T. Zahir, C. H. Tator, and M. S. Shoichet, "Effects of dibutyryl cyclic-AMP on survival and neuronal differentiation of neural stem/progenitor cells transplanted into spinal cord injured rats," *PLoS One*, vol. 6, no. 6, 2011.

[43] H. Cheng, Y. Cao, and L. Olson, "Spinal cord repair in adult paraplegic rats: partial restoration of hind limb function.," *Science*, vol. 273, no. 5274, pp. 510–513, 1996.

[44] C. D. Pritchard, J. R. Slotkin, D. Yu, H. Dai, M. S. Lawrence, R. T. Bronson, F. M. Reynolds, Y. D. Teng, E. J. Woodard, and R. S. Langer, "Establishing a model spinal cord injury in the African green monkey for the preclinical evaluation of biodegradable polymer scaffolds seeded with human neural stem cells," *J. Neurosci. Methods*, vol. 188, no. 2, pp. 258–269, 2010.

[45] Y. tae Kim, J. M. Caldwell, and R. V. Bellamkonda, "Nanoparticle-mediated local delivery of methylprednisolone after spinal cord injury," *Biomaterials*, vol. 30, no. 13, pp. 2582–2590, 2009.

[46] C. A. Tobias, S. S. W. Han, J. S. Shumsky, D. Kim, M. Tumolo, N. O. Dhoot, M. A. Wheatley, I. Fischer, A. Tessler, and M. Murray, "Alginate encapsulated BDNF-producing fibroblast grafts permit recovery of function after spinal cord injury in the absence of immune suppression.," *J. Neurotrauma*, vol. 22, no. 1, pp. 138–156, 2005.

[47] E. Trovatti, C. S. R. Freire, P. C. Pinto, I. F. Almeida, P. Costa, A. J. D. Silvestre, C. P. Neto, and C. Rosado, "Bacterial cellulose membranes applied in topical and transdermal delivery of lidocaine hydrochloride and ibuprofen: In vitro diffusion studies," *Int. J. Pharm.*, vol. 435, no. 1, pp. 83–87, Oct. 2012.

[48] L. Basiricò, P. Cosseddu, A. Scidà, B. Fraboni, G. G. Malliaras, and A. Bonfiglio, "Electrical characteristics of ink-jet printed, all-polymer electrochemical transistors," *Org. Electron.*, vol. 13, no. 2, pp. 244–248, Feb. 2012.

[49] R. G. Tremblay, M. Sikorska, J. K. Sandhu, P. Lanthier, M. Ribecco-Lutkiewicz, and M. Bani-Yaghoub, "Differentiation of mouse Neuro 2A cells into dopamine neurons," *J. Neurosci. Methods*, vol. 186, no. 1, pp. 60–67, Jan. 2010.

[50] B. a Barres, "New roles for glia.," *J. Neurosci.*, vol. 11, no. 12, pp. 3685–3694, 1991.

[51] A. Verkhratsky and H. Kettenmann, "Calcium signalling in glial cells," *Trends in Neurosciences*, vol. 19, no. 8. pp. 346–352, Aug-1996.

[52] A. Verkhratsky and C. Steinhäuser, "Ion channels in glial cells.," *Brain Res. Brain Res. Rev.*, vol. 32, no. 2–3, pp. 380–412, Apr. 2000.

[53] E. Barsoukov and J. R. Macdonald, *Impedance Spectroscopy*. Hoboken, NJ, USA: John Wiley & Sons, Inc., 2005.

[54] F. Asphahani, K. Wang, M. Thein, O. Veiseh, S. Yung, J. Xu, and M. Zhang, "Single-cell bioelectrical impedance platform for monitoring cellular response to drug treatment," *Phys. Biol.*, vol. 8, no. 1, p. 015006, Feb. 2011.

[55] S. Vogler, A. Grosche, T. Pannicke, E. Ulbricht, P. Wiedemann, A. Reichenbach, and A. Bringmann, "Hypoosmotic and glutamate-induced swelling of bipolar

cells in the rat retina: Comparison with swelling of Müller glial cells," *J. Neurochem.*, vol. 126, no. 3, pp. 372–381, Aug. 2013.

[56] M. Erecińska, D. Nelson, F. Dagani, J. Deas, and I. A. Silver, "Relations between intracellular ions and energy metabolism under acidotic conditions: a study with nigericin in synaptosomes, neurons, and C6 glioma cells.," *J. Neurochem.*, vol. 61, no. 4, pp. 1356–1368, 1993.

[57] D. Kim, B. Goldstein, W. Tang, F. J. Sigworth, and E. Culurciello, "Noise analysis and performance comparison of low current measurement systems for biomedical applications," *IEEE Trans. Biomed. Circuits Syst.*, vol. 7, no. 1, pp. 52–62, 2013.

[58] M. Crescentini, M. Bennati, M. Carminati, and M. Tartagni, "Noise limits of CMOS current interfaces for biosensors: A review," *IEEE Trans. Biomed. Circuits Syst.*, vol. 8, no. 2, pp. 278–292, Apr. 2014.

[59] M. Hutzler and P. Fromherz, "Silicon chip with capacitors and transistors for interfacing organotypic brain slice of rat hippocampus," *Eur. J. Neurosci.*, vol. 19, no. 8, pp. 2231–2238, Apr. 2004.

[60] H. Sontheimer, "Voltage-dependent ion channels in glial cells.," *Glia*, vol. 11, no. 2, pp. 156–172, Jun. 1994.

[61] U. Pannasch, M. Derangeon, O. Chever, and N. Rouach, "Astroglial gap junctions shape neuronal network activity," *Commun. Integr. Biol.*, vol. 5, no. 3, pp. 248–254, May 2012.

[62] R. Zorec, A. Araque, G. Carmignoto, P. G. Haydon, A. Verkhratsky, and V. Parpura, "Astroglial excitability and gliotransmission: an appraisal of Ca 2+ as a signalling route," *ASN Neuro*, vol. 4, no. 2, pp. 103–119, Mar. 2012.

[63] T. Brismar, "Physiology of transformed glial cells.," *Glia*, vol. 15, no. 3, pp. 231–243, Nov. 1995.

[64] J. Pallud, L. Capelle, and G. Huberfeld, "Tumoral epileptogenicity: How does it happen'," *Epilepsia*, vol. 54, no. SUPPL. 9, pp. 30–34, Dec. 2013.

[65] G. T. A. Kovacs, "Electronic sensors with living cellular components," *Proc. IEEE*, vol. 91, no. 6, pp. 915–929, Jun. 2003.

[66] F. Heer, S. Hafizovic, T. Ugniwenko, U. Frey, W. Franks, E. Perriard, J. C. Perriard, A. Blau, C. Ziegler, and A. Hierlemann, "Single-chip microelectronic system to interface with living cells," *Biosens. Bioelectron.*, vol. 22, no. 11, pp. 2546–2553, May 2007.

[67] I. Schoen and P. Fromherz, “The mechanism of extracellular stimulation of nerve cells on an electrolyte-oxide-semiconductor capacitor.,” *Biophys. J.*, vol. 92, no. 3, pp. 1096–1111, Feb. 2007.

[68] L. Leybaert and M. J. Sanderson, “Intercellular Ca2+ Waves: Mechanisms and Function,” *Physiological Reviews*, vol. 92, no. 3. pp. 1359–1392, 01-Jul-2012.

[69] M. Giacomello, R. Hudec, and R. Lopreiato, “Huntington’s disease, calcium, and mitochondria,” *BioFactors*, vol. 37, no. 3. pp. 206–218, May-2011.

[70] A. A. Webb, S. Ngan, and J. D. Fowler, “Spinal cord injury I: A synopsis of the basic science.,” *Can. Vet. J.*, vol. 51, no. 5, pp. 485–492, Oct. 2010.

[71] T. D. Hassinger, P. B. Guthrie, P. B. Atkinson, M. V Bennett, and S. B. Kater, “An extracellular signaling component in propagation of astrocytic calcium waves.,” *Proc. Natl. Acad. Sci. U. S. A.*, vol. 93, no. 23, pp. 13268–13273, Nov. 1996.

[72] H. Helmholtz, “Studien über electrische Grenzschichten,” *Ann. der Phys. und Chemie*, vol. 243, no. 7, pp. 337–382, 1879.

[73] O. Stern, “Zur Theorie der Elektrolytischen Doppelschicht,” *Zeitschrift fur Elektrochemie*, vol. 30, pp. 508–516, 1924.

[74] R. Gleixner and P. Fromherz, “The extracellular electrical resistivity in cell adhesion.,” *Biophys. J.*, vol. 90, no. 7, pp. 2600–2611, Apr. 2006.

[75] B. Ordaz, L. Vaca, R. Franco, and H. Pasantes-Morales, “Volume changes and whole cell membrane currents activated during gradual osmolarity decrease in C6 glioma cells: contribution of two types of K+ channels.,” *Am. J. Physiol. Cell Physiol.*, vol. 286, no. 6, pp. C1399–C1409, Jun. 2004.

[76] S. L. Campbell, S. C. Buckingham, and H. Sontheimer, “Human glioma cells induce hyperexcitability in cortical networks,” *Epilepsia*, vol. 53, no. 8, pp. 1360–1370, Aug. 2012.

[77] S. M. Z. Hossain, H. Shinohara, F. Wang, and H. Kitano, “Real-time detection of L-glutamate released from C6 glioma cells using a modified enzyme-luminescence method,” *Anal. Bioanal. Chem.*, vol. 389, no. 6, pp. 1961–1966, Oct. 2007.

[78] M. Strupp, F. Staub, and P. Grafe, “A Ca(2+)- and pH-dependent K+ channel of rat C6 glioma cells and its possible role in acidosis-induced cell swelling.,” *Glia*, vol. 9, no. 2, pp. 136–145, 1993.

[79] N. Kapoor, R. Bartoszewski, Y. J. Qadri, Z. Bebok, J. K. Bublen, C. M. Fuller, and D. J. Benos, “Knockdown of ASIC1 and epithelial sodium channel subunits

inhibits glioblastoma whole cell current and cell migration," *J. Biol. Chem.*, vol. 284, no. 36, pp. 24526–24541, Sep. 2009.

[80] A. K. Rooj, C. M. McNicholas, R. Bartoszewski, Z. Bebok, D. J. Benos, and C. M. Fuller, "Glioma-specific cation conductance regulates migration and cell cycle progression," *J. Biol. Chem.*, vol. 287, no. 6, pp. 4053–4065, Feb. 2012.

[81] W. H. Vila-Carriles, G. G. Kovacs, B. Jovov, Z. H. Zhou, A. K. Pahwa, G. Colby, O. Esimai, G. Y. Gillespie, T. B. Mapstone, J. M. Markert, C. M. Fuller, J. K. Bubien, and D. J. Benos, "Surface expression of ASIC2 inhibits the amiloride-sensitive current and migration of glioma cells," *J. Biol. Chem.*, vol. 281, no. 28, pp. 19220–19232, May 2006.

[82] X. C. Weng, J. Q. Zheng, J. Li, and W. B. Xiao, "Underlying mechanism of ASIC1a involved in acidosis-induced cytotoxicity in rat C6 glioma cells," *Acta Pharmacol. Sin.*, vol. 28, no. 11, pp. 1731–1736, Nov. 2007.

[83] P. Swietach, A. Hulikova, R. D. Vaughan-Jones, and A. L. Harris, "New insights into the physiological role of carbonic anhydrase IX in tumour pH regulation.," *Oncogene*, vol. 29, no. 50, pp. 6509–6521, Dec. 2010.

[84] E. Grillon, R. Farion, K. Fablet, M. de Waard, C. M. Tse, M. Donowitz, C. Rémy, and J. A. Coles, "The spatial organization of proton and lactate transport in a rat brain tumor," *PLoS One*, vol. 6, no. 2, p. e17416, Feb. 2011.